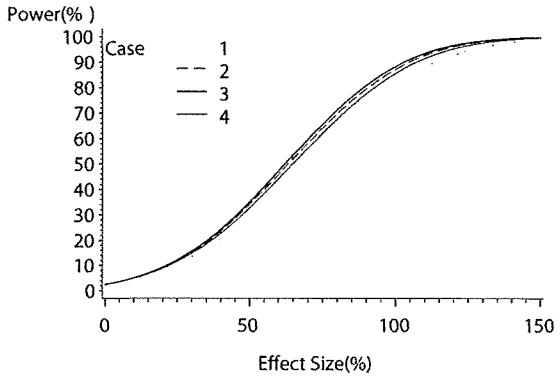

Figure 4. Relation between power and group size in four cases

4.3.1. Fixed conditions.

1. Group points for single administration: $(d_A, d_B) = (0, 0), (1, 0), (2, 0), (0, 1), (0, 2)$.
2. Group point for simultaneous administration: $(d_A, d_B) = (0.6, 0.6)$.
3. Parameters in the dose–response curve: $\beta_0 = 1.0$, $\beta_A = 1.0$, $\beta_B = 1.0$.
4. Variance σ^2: $\sigma_s^2 = \sigma_m^2 = 1.0$.
5. Nominal significance level of t-test: one-sided 2.5%.
6. Total number of animals: $n = 42$.

4.3.2. Varied conditions.

7. Group size:
   Case 1: $n_s = 6, n_m = 12$
   Case 2: $n_s = 5, n_m = 17$
   Case 3: $n_s = 4, n_m = 22$
   Case 4: $n_s = 3, n_m = 27$
8. Effect Size: $\Delta/\sigma_m = 0.1(0.1)1.5$.

Figure 4 shows the results of the numerical calculations, with the power on the vertical axis and the effect size on the horizontal axis. According to Figure 4, regardless of the effect size, Case 3 gives the maximum power. Because the group size is constrained to be an integer, it is not possible to give the most appropriate group size as a continuous value. The power becomes larger when the group size of the simultaneous administration group is set larger than that of the single administration group. When $n = 42$, what is prominent is the fact that the group size of 22 in the simultaneous administration group is nearly equal to the total number of animals in the single administration group, $4 \times 5 = 20$.

5. DISCUSSION

5.1. Conclusion under assumed conditions

In the previous section, we investigated applicable designs assuming that the response variables follow a homoscedastic normal distribution, that the dose–response relationship for single administration is

DOI: 10.1002/env

linear, that synergism is defined as a larger response obtained with simultaneous administration as compared to the dose plane obtained with single administration by assuming additivity, that there are five groups for single administration and one group for simultaneous administration, etc.

As the results of numerical calculation for the group point, when the departure Δ from additivity is proportional to square root of the dose, it is revealed that the group point for the simultaneous administration group should be on the boundary of the triangle region. Here, the results seemed to be reasonable. Because it is natural to expect that the departure Δ does not continue to increase along with the dose constantly. So, we applied these two situations as the sensitivity analysis. When the departure Δ become larger linearly along with the dose, the group point should be located slightly outside the triangle region. On the other hand, the group point should be set inside the triangle region when the departure Δ is constant. However, the group point should be placed on the boundary of the triangular region, because the reduction of power from a recommended group point is small. This means that the conventional design in the real study is appropriate.

Subsequently, with respect to the group size, we revealed that the total number of animals allocated to the simultaneous administration group should be same size as that in the single administration group.

5.2. *Heteroscedasticity*

When heteroscedasticity in data is expected from the past research, it is required to adjust the degree of freedom by using the Welch test. For the cases discussed in this paper, we used the Welch test, which is robust for heteroscedasticity because there is a tendency in real data for the variance to increase with an increase in responses although the number of animals is small. However, the Welch test does not control a type 1 error below the nominal significance level under heteroscedasticity. It is, therefore, required to confirm, *ex post facto*, the type 1 error when the degree of heteroscedasticity is large.

5.3. *Linearity*

For the cases discussed in this paper, based on advanced information, it was possible to select the dose so that there is linearity with the single administration group. This was easier due to the fact that the number of dose levels in the single administration group was small (three levels). From the experimental results, it was also confirmed that the linearity assumptions were established to some extent. When using the results in this paper, it is important to confirm the dose–response relationship in preliminary experiments or in past experiments using analogous substances. It is necessary to examine, *ex post facto*, the linearity by displaying in figure or by linearity tests.

5.4. *Group size*

The group size must be an integer of at least 1. In addition, the total number of animals must be a comparatively small. Under these conditions, as in this paper, it is necessary to obtain the appropriate design using numerical calculations, separately considering a combination of possible group sizes. However, in order to generalize these results, it is useful to perform power calculations, taking the group size as a continuous value. When calculating the recommended ratio of the total number of animals in the single administration group to the group size of the simultaneous administration group, the results shown in Figure 5 are obtained.

When determining the appropriate group point of the simultaneous administration group, with the departure Δ from the additivity being constant, the highest power is obtained by setting the number of

DOI: 10.1002/env

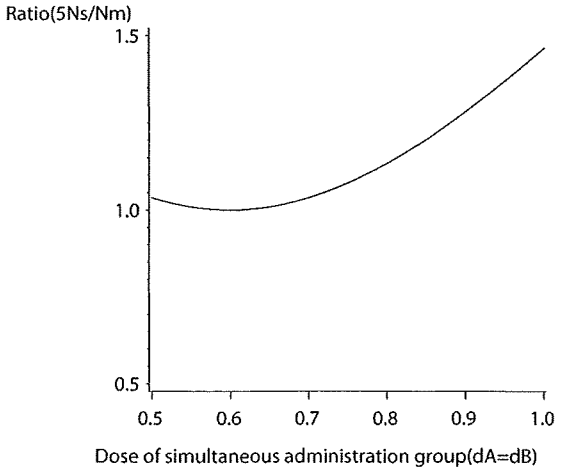

Figure 5. Recommended ratio of the group size between single administration group and simultaneous administration group

animals at a ratio of 1:1 between the single administration group and the simultaneous administration group.

When determining the simultaneous administration group on the boundary of the triangular region, a theoretical calculation shows that the allocation at a ratio of 1.464:1 is appropriate. In other words, it is best to set the total number of animals in the single administration group to be approximately 1.5 times the total number of animals in the simultaneous administration group. The reason is that because it is theoretically favorable for the accuracy of estimates based on additivity to be equal to that based on simultaneous administration.

5.5. Practical consideration on the recommended design

In the numerical examples of the previous section, we showed that the group point for the simultaneous administration on the boundary of the triangular region is not necessarily best and the recommended number of animals for the simultaneous administration group is considerably greater than those for single administration groups.

Although these results speciously imply that the design exemplified in the Subsection 4.1 should be replaced with the recommended design shown in this paper in future, we think it is not always true, because we have to take practical conditions into consideration, which were not incorporated in the assumptions to derive the recommended design.

One of them is the robustness or stability of the result of data analysis in such experiments. The situation is quite similar to that for the recommended design at linear regression analysis, for example, related to a single chemical experiment. Actually, if we can entirely assume the linearity of the dose–response relationship in regression analysis, the recommended design is to allocate a half of animals to the maximum dose and the remaining half to the minimum dose, while such design is really not adopted and animals are evenly allocated to uniformly distributed three or four doses probably to secure the robustness of the result of data analysis. Likewise, when the functional relationship of the Δ is not particularly clear, or when there is concern for the instability in squeezing the simultaneous administration group into one group in our experiments, the design with two or three simultaneous

DOI: 10.1002/env

administration groups within the triangular region must be practical. Since the mathematical formulation in such condition could not be established up to present due to its difficult nature, we left it for future investigation.

5.6. *Other issues for future investigation*

When the number of test substances is 3 or more, there needs to be strict controls for the number of required animals. Therefore, a design must be determined by examining the design conditions in detail for each case. Under this condition, an investigation following the same approach as in this paper is necessary. This is another problem to be addressed in future research.

In this paper, we introduced a test statistic by using the unweighted least squares method. The weighted least squares method must be considered when the rules for the size of variance are understood from past research, such that variance linearly becomes larger along with the dose. The specific design in this instance is also to be investigated in the future.

ACKNOWLEDGMENT

We thank Professor Takashi Sozu at Osaka University for his assistance in the preparation of this paper. We are grateful to the Editor-in-Chief and two anonymous reviewers for their comments that greatly improved this paper.

REFERENCES

Abdelbasit KM, Plackett RL. 1982. Experimental design for joint action. *Biometrics* **38**: 171–179.

Berenbaum MC. 1989. What is synergy? *Pharmacological Review* **41**: 93–141.

Gennings C, Schwartz P, Carter WH, Simmons JE. 1997. Detection of departures from additivity in mixtures of many chemicals with a threshold model. *Journal of Agricultural, Biological, and Environmental Statistics* **2**: 198–211.

Gennings C, Carter WH. 1995. Utilizing concentration-response data from individual components to detect statistically significant departures from additivity in chemical mixture. *Biometrics* **51**: 1264–1277.

Hasegawa R, Yoshimura I, Imaida K, Ito N, Shirai T. 1996. Analysis of synergism in hepatocarcinogenesis based on preneoplastic foci induction by 10 heterocyclic amines in the rat. *Japanese Journal of Cancer Research* **87**: 1125–1133.

Hewlett PS, Plackett RL. 1959. A unified theory for quantal response to mixtures of drugs: noninteractive action. *Biometrics* **15**: 591–610.

Kanno J, Onyon L, Haseman J, Fenner-Crisp P, Axhby J, Owens W. 2001. The OECD program to validate the rat uterotrophic bioassay to screen compounds for *in vivo* estrogenic response: phase 1. *Environmental Health Perspectives* **109**: 785–794.

Kelly C, Rice J. 1990. Monotone smoothing with application to dose-response curve and the assessment of synergism. *Biometrics* **46**: 1071–1085.

Laska EM, Meisner MJ. 1989. Testing whether an identified treatment is best. *Biometrics* **45**: 1139–1151.

Matsunaga N, Kanno J, Yoshimura I. 2003. A statistical method for judging synergism application to an endocrine disruptor animal experiment. *Environmetrics* **14**: 213–222.

Machado SG, Robinson GA. 1994. A direct, general approach based on isobologram for assessing the joint action of drugs in pre-clinical experiment. *Statistics in Medicine* **13**: 2289–2309.

Roy P, Esteve J. 1998. Using relative risk models for estimating synergy between two risk factors. *Statistics in Medicine* **17**: 1357–1373.

Straetemans R, O'Brien T, Wouters L, Dun JV, Janicot M, Bijnens L, Burzykowski T, Aerts M. 2005. Design and analysis of drug combination experiments. *Biometrical Journal* **47**: 299–308.

Tan M, Fang HB, Tian GL, Houghton PJ. 2003. Experimental design and sample size determination for testing synergism in drug combination studies based on uniform measures. *Statistics in Medicine* **22**: 2091–2100.

Neonatal Exposure to Low-Dose 2,3,7,8-Tetrachlorodibenzo-*p*-Dioxin Causes Autoimmunity Due to the Disruption of T Cell Tolerance[1]

Naozumi Ishimaru,* Atsuya Takagi,† Masayuki Kohashi,* Akiko Yamada,* Rieko Arakaki,* Jun Kanno,† and Yoshio Hayashi[2]*

Although 2,3,7,8-tetrachlorodibenzo-*p*-dioxin (TCDD) has been shown to influence immune responses, the effects of low-dose TCDD on the development of autoimmunity are unclear. In this study, using NFS/*sld* mice as a model for human Sjögren's syndrome, in which the lesions are induced by the thymectomy on day 3 after birth, the autoimmune lesions in the salivary glands, and in later phase, inflammatory cell infiltrations in the other organs were developed by neonatal exposure to nonapoptotic dosage of TCDD without thymectomy on day 3 after birth. We found disruption of thymic selection, but not thymic atrophy, in TCDD-administered mice. The endogenous expression of aryl hydrocarbon receptor in the neonatal thymus was significantly higher than that in the adult thymus, suggesting that the neonatal thymus may be much more sensitive to TCDD compared with the adult thymus. In addition, the production of T_H1 cytokines such as IL-2 and IFN-γ from splenic $CD4^+$ T cells and the autoantibodies relevant for Sjögren's syndrome in the sera from TCDD-exposed mice were significantly increased compared with those in control mice. These results suggest that TCDD/aryl hydrocarbon receptor signaling in the neonatal thymus plays an important role in the early thymic differentiation related to autoimmunity. *The Journal of Immunology,* 2009, 182: 6576–6586.

The toxicity of 2,3,7,8-tetrachlorodibenzo-*p*-dioxin (TCDD),[3] the environmental contaminant, has been shown to influence various biological responses such as immunological, reproductive, and neurobehavioral (1–3). It has been reported that TCDD induces thymic atrophy and suppresses a variety of T cell-dependent immune responses, including delayed-type and contact hypersensitivity responses and the activity of CTL itself (4–7). However, TCDD has been shown to enhance the proliferation and cytokine production of mitogen- or Ag-stimulated T cells (8). In this context, when a DO11.10 transgenic T cell model was used to investigate the effects of TCDD on the activation of Ag-specific $CD4^+$ T cells by transfer of $CD4^+$ T cells into TCDD-treated recipient mice, the exposure to TCDD had little effect on the initial activation, but on day 3 after OVA-peptide injection the T cell proliferation of TCDD-treated recipients was enhanced compared with that of control recipients (9). Thus, the effect of TCDD seems to be dependent on the developmental state and active state of the T cells. As for the effects of TCDD on B cells, it was reported that TCDD inhibited B cell proliferation triggered by LPS, surface Ig cross-linking, or PMA/ionomycin (10, 11). Moreover, the in vivo suppressive effect of TCDD on T cell-dependent Ab response to sheep RBC (SRBC) was found as an immunotoxicity of TCDD (12). However, the effects of TCDD on autoimmunity or on autoantibody production in autoimmune animal models have not been demonstrated.

A combination of immunologic, genetic, and environmental factors may play a key role on the development of autoimmune disease, which is induced by the breakdown of central or peripheral tolerance (13–15). Sjögren's syndrome (SS) is generally considered to be a T cell-mediated autoimmune disorder characterized by lymphocytic infiltrates and destruction of the exocrine glands, particularly of the salivary glands, and systemic production of autoantibodies against the ribonucleoprotein particles SS-A/Ro and SS-B/La (16–18). We have established and analyzed an animal model for SS in NFS/*sld* mutant mouse thymectomized 3 days after birth (3d-Tx) (19–21). It is well established that 3d-Tx in a certain strain of mice results in spontaneous development of inflammatory lesions similar to human autoimmune diseases in the thyroid, ovary, kidney, testis, and stomach, but little is known about the mechanisms leading to the induction of autoimmunity (22–25). From the findings in 3d-Tx autoimmune models, the initiation of autoreactivity is thought to be due to the retardation of regulatory T (Treg) cell differentiation together with lymphopenia caused by neonatal thymectomy. In other words, the impairment of T cell differentiation and/or maturation in the neonatal thymus may cause the initiation of T cell self-reactivity. Although the perinatal exposure to TCDD has been shown to induce the suppression of cell-mediated immunity to a more severe degree than those in adult exposure, the association of neonatal exposure to TCDD with the development of autoimmunity remains unclear (5, 6).

*Department of Oral Molecular Pathology, Institute of Health Biosciences, University of Tokushima Graduate School, Kuramotocho, Tokushima, Japan; and †Division of Cellular and Molecular Toxicology, Biological Safety Research Center, National Institute of Health Sciences, Kamiyoga, Setagayaku, Tokyo, Japan

Received for publication July 14, 2008. Accepted for publication March 17, 2009.

The costs of publication of this article were defrayed in part by the payment of page charges. This article must therefore be hereby marked *advertisement* in accordance with 18 U.S.C. Section 1734 solely to indicate this fact.

[1] This work was supported by a Health Sciences Research Grant (H17, 18, and 19-kagaku-ippan-003) from the Ministry of Health, Labor and Welfare, Japan and a Grant-in-Aid for Scientific Research (no. 17109016) from the Ministry of Education, Culture, Sports, Science and Technology of Japan.

[2] Address correspondence and reprint requests to Dr. Yoshio Hayashi, Department of Oral Molecular Pathology, Institute of Health Biosciences, University of Tokushima Graduate School, 3-18-15 Kuramotocho, Tokushima 770-8504, Japan. E-mail address: hayashi@dent.tokushima-u.ac.jp

[3] Abbreviations used in this paper: TCDD, 2,3,7,8-tetrachlorodibenzo-*p*-dioxin; 3d-Tx, thymectomized 3 days after birth; AhR, aryl hydrocarbon receptor; AIRE, autoimmune regulator; ARNT, AhR nuclear translocator; DN, double negative; DP, double positive; DRE, dioxin responsive element; IRF, IFN regulatory factor; SP, single positive; SS, Sjögren's syndrome; TEC, thymic epithelial cell; Treg, regulatory T; XRE, xenobiotic response element.

www.jimmunol.org/cgi/doi/10.4049/jimmunol.0802289

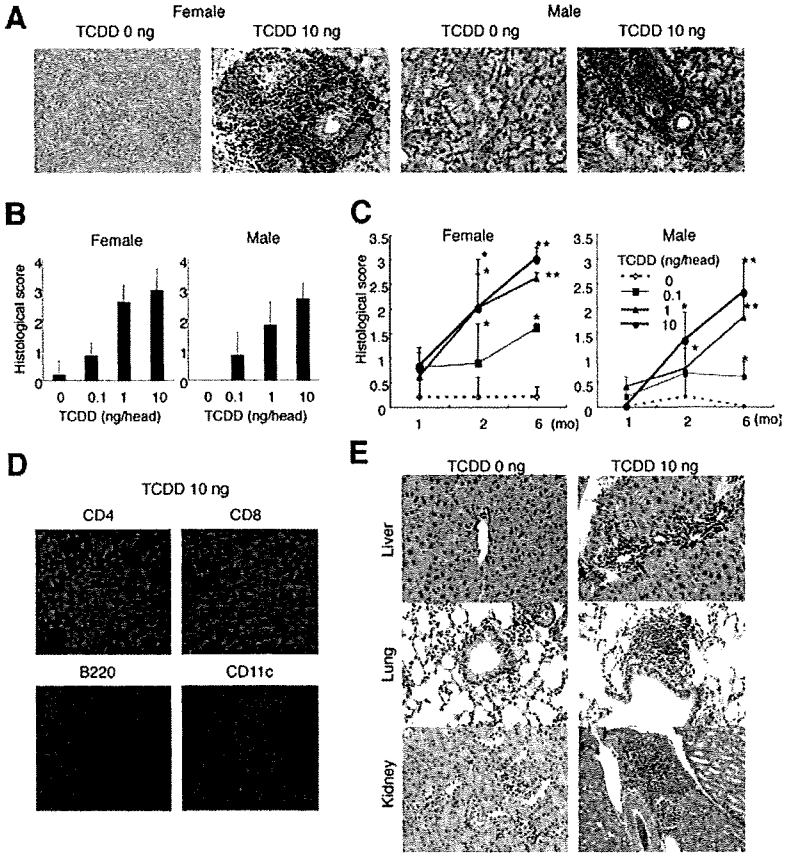

FIGURE 1. Inflammatory lesions induced by neonatal exposure to low-dose TCDD. *A*, Histology of salivary glands in female and male mice (6 mo) treated with 0 and 10 ng of TCDD were shown. H&E staining was performed using paraffin-embedded sections. Photos are representative of five to seven mice in each group. *B*, Histological score of the salivary glands at 6 mo of age was evaluated using the sections stained with H&E. Results are shown as the mean ± SD in the five to seven mice in each group. *C*, The change of inflammatory lesions from 1 to 6 mo of age in female and male mice treated with low-dose TCDD. Results are shown as the mean ± SD in the five to seven mice in each group. *, $p < 0.05$; **, $p < 0.005$. *D*, Immune cells in the inflammatory lesions of salivary glands from TCDD-treated mice at 6 mo of age were analyzed by immunofluorescence staining using anti-CD4, CD8, B220, and CD11c mAbs with Alexa Fluor 568-conjugated rat IgG (H+L) as the secondary Abs. Nuclei were stained with 4′,6-diamidino-2-phenylindole. Photos are representative of three to five sections in each group. *E*, Inflammatory lesions of liver, lung, and kidney induced by TCDD treatment. The sections from TCDD-treated mice at 6 mo of age were stained with H&E. Photos are representative of five to seven mice in each group.

One mechanism of TCDD action is binding and activation of the aryl hydrocarbon receptor (AhR) (1, 26). The AhR is a cytosolic transcription factor of the basic helix-loop-helix family. The activated receptor heterodimerizes with the AhR nuclear translocator (ARNT) in the nucleus and binds the xenobiotic response elements (XREs), also known as dioxin responsive elements (DREs), and alters the expressions of various genes such as cytochrome P450 1A1 (CYP1A1). TCDD, via the AhR, has been shown to have a variety of effects on T cell development and function, including decreasing the number of thymocytes by apoptosis and altering the effector functions of mature Th and T killer cells (27–30). Although a variety of studies have been performed to determine how high-dose TCDD is influencing T cells and the thymus (29–31), the mechanism and targets of its actions are still unclear. In addition, TCDD also induced the binding of several NF-κB proteins to a κB site, one of which overlapped with a DRE site (32). It has been uncertain whether the neonatal exposure to low-dose TCDD in vivo influences the TCDD signaling including AhR, CYP1A1, or NF-κB of immune cells.

In this study, we evaluated whether the immunotoxicity of nonapoptotic and low-dose TCDD during neonatal period influences the development of autoimmune disease in the murine SS-susceptible strain. Moreover, the correlation between the TCDD-induced signaling pathway in neonatal T cells and the initiation of self-reactivity in vivo was analyzed.

Materials and Methods

Mice

NFS/N strain carrying the mutant gene *sld* was reared in our specific pathogen-free mouse colony, and given food and water ad libitum. Experiments were humanely conducted under the regulation and permission of the Animal Care and Use Committee of the National Institute of Health Sciences, Tokyo, Japan and the University of Tokushima, Tokushima, Japan.

Neonatal administration of TCDD

Intraperitoneal injection of 10 μl of corn oil including TCDD (0, 0.1, 1, or 10 ng/mouse) with neonatal mice was performed on day 0, 1, and 2 after birth. Treatment of TCDD and TCDD-injected mice followed the rules of the National Institute of Health Sciences.

Histology

All organs were removed from the mice, fixed with 4% phosphate-buffered formaldehyde (pH 7.2), and prepared for histologic examination. Formalin-fixed tissue sections were subjected to H&E staining, and three pathologists independently evaluated the histology without being informed of the condition of each individual mouse. Histological changes were scored according to the method proposed by White and Casarett (33), as follows: 1 = 1–5 foci composed of >20 mononuclear cells per focus; 2 = >5 such foci, but without significant parenchymal destruction; 3 = degeneration of parenchymal tissue; 4 = extensive infiltration of the glands with mononuclear cells and extensive parenchymal destruction. Histological evaluation was performed in a blinded manner, and one tissue section from each salivary and lacrimal gland was examined.

Confocal microscopic analysis

Frozen sections were stained with 1 μg/ml primary Abs against CD4, CD8, B220, and CD11b/c (eBioscience) for 1 h. After three washes in PBS, the sections were stained with Alexa Fluor 568 donkey anti-rat IgG (H+L) (Molecular Probes) as the second Abs for 30 min and washed with PBS. The nuclei was stained with 4′,6-diamidino-2-phenylindole. The sections were visualized with a laser scanning confocal microscope (Carl Zeiss). A 63 × 1.4 oil differential interference contrast objective lens was used. Quick Operation Version 3.2 (Carl Zweiss) for imaging acquisition and Adobe Photoshop CS2 (Adobe System) for image processing was used.

Table I. *Incidence of inflammatory lesions in TCDD-treated mice*

	Female			Male		
	1 mo	2 mo	6 mo	1 mo	2 mo	6 mo
Liver treated with TCDD (ng)						
0	0/5 (0)	0/7 (0)	0/5 (0)	0/6 (0)	0/6 (0)	0/9 (0)
0.1	0/6 (0)	2/8 (25)	2/5 (40)	0/5 (0)	0/6 (0)	2/6 (33)
1	1/5 (20)	2/6 (33)	1/6 (17)	4/8 (50)	0/6 (0)	2/6 (33)
10	2/5 (40)	3/6 (50)	2/6 (33)	2/6 (33)	4/6 (67)	5/7 (71)
Lung treated with TCDD (ng)						
0	0/5 (0)	0/7 (0)	1/6 (17)	0/6 (0)	0/7 (0)	0/9 (0)
0.1	0/6 (0)	4/8 (50)	3/5 (60)	0/5 (0)	0/5 (0)	3/6 (50)
1	1/5 (20)	2/6 (33)	4/6 (67)	2/8 (25)	3/6 (50)	6/6 (100)
10	2/5 (40)	3/6 (50)	6/6 (100)	1/6 (17)	6/6 (100)	7/7 (100)
Kidney treated with TCDD (ng)						
0	0/5 (0)	0/7 (0)	0/6 (0)	0/6 (0)	0/7 (0)	0/9 (0)
0.1	0/6 (0)	0/8 (0)	1/5 (20)	1/5 (20)	3/5 (60)	4/6 (67)
1	0/5 (0)	0/6 (0)	2/6 (33)	2/8 (25)	4/6 (67)	5/6 (83)
10	1/5 (20)	3/6 (50)	2/6 (33)	2/6 (33)	6/6 (100)	5/7 (71)

The incidence of inflammatory lesions in the liver, lung, and kidney was histologically evaluated using the H&E-stained sections of the TCDD-treated NFS/*sld* mice at 1, 2, and 6 mo of age. The number of inflammatory lesion-induced mice in the organ/the total number of treated mice (%) is indicated.

Flow cytometric analysis

Surface markers were identified by mAbs with BD FACSCant flow cytometer (BD Biosciences). Rat mAbs to FITC-, PE-, or PE-Cy5-conjugated anti-B220, Thy1.2, CD4, CD8, CD25, and CD44 mAbs (eBioscience) were used. Intracellular Foxp3 expression was analyzed with an intracellular Foxp3 detection kit (eBioscience) according to the manufacturer's instructions. For intracellular AhR expression, cells were stained with PE-Cy5.5-conjugated anti-CD4, PE-conjugated anti-CD8, PE-Cy7-conjugated anti-CD44, allophycocyanin-conjugated anti-CD25 mAbs, and then fixed in fixation/permeabilization solution (eBioscience) for 18 h at 4°C. After washing twice with the permeabilization buffer (eBioscience), the cells were blocked with Fc block for 40 min on ice, and incubated in rabbit anti-AhR polyclonal Ab (BIOMOL) for 2 h at 4°C. After washing with the permeabilization buffer, the cells were stained with FITC-conjugated ant-rabbit IgG for 30 min at 4°C for flow cytometric analysis of multicolors. The data were analyzed with FlowJo FACS Analysis software (Tree Star).

Proliferation assay

Cell proliferation was evaluated by counting of divisions by CFSE (Molecular Probes) dilution of labeled cells. After stimulation by anti-CD3 and

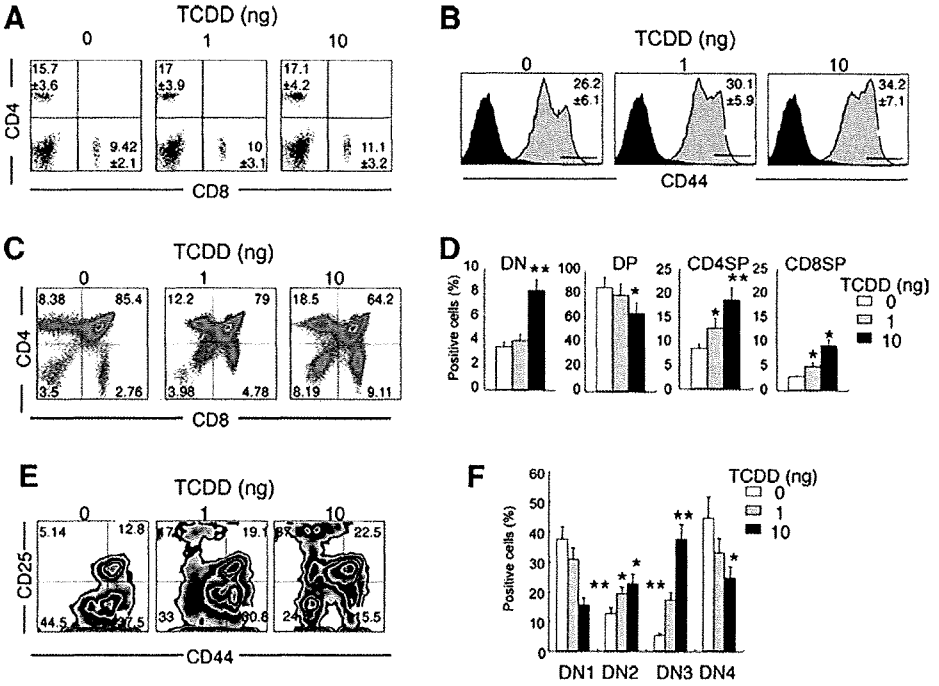

FIGURE 2. The effect of in vivo TCDD injection on T cell phenotypes. *A*, CD4 and CD8 expressions on spleen cells from female TCDD-treated mice at 6 mo of age were analyzed by flow cytometry. Positive cells (%) were indicated as the mean ± SD of five to seven mice in each group. *B*, CD44 expression on $CD4^+$ T cells in spleen from TCDD-treated mice. $CD44^{high}$ cells (%) are indicated as the mean ± SD of five to seven mice in each group. *C*, T cell differentiation in thymus of TCDD-treated mice was analyzed by flow cytometry using CD4 and CD8 expressions. Figures are representative of five to seven mice in each group. *D*, T cell population in thymus. $CD4^-CD8^-$ DN, $CD4^+CD8^+$ DP, $CD4^+CD8^-$ SP (CD4SP), and $CD4^-CD8^+$ SP (CD8SP) cells (%) are shown as the mean ± SD of five to seven mice in each group. *E*, The differentiation of DN T cells was evaluated using CD44 and CD25 expressions. Figures are representative of five to seven mice in each group. *F*, $CD44^+CD25^-$ (DN1), $CD44^+CD25^+$ (DN2), $CD44^-CD25^+$ (DN3), and $CD44^-CD25^-$ (DN4) cells (%) are shown as the mean ± SD of five to seven mice in each group. *, $p < 0.05$; **, $p < 0.005$.

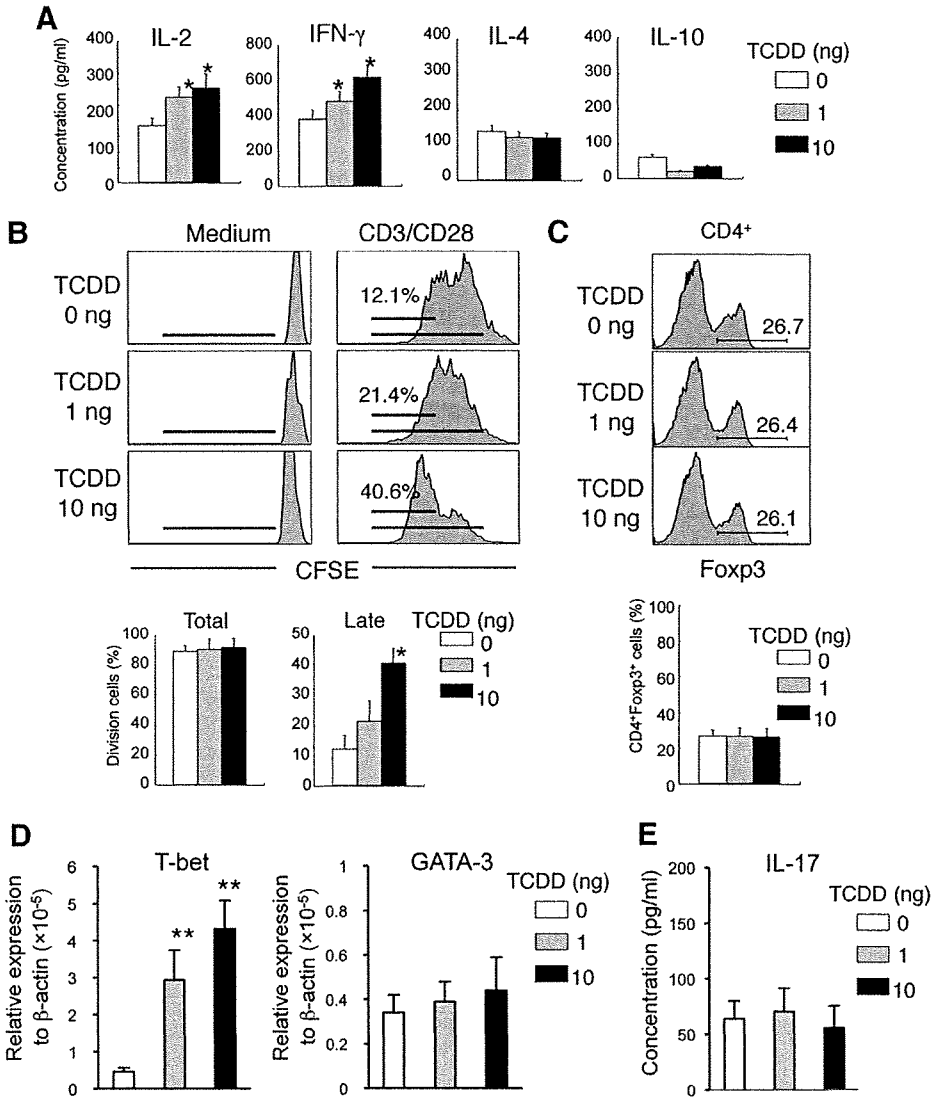

FIGURE 3. T cell functions in low-dose TCDD-treated mice. *A*, T_H1 and T_H2 type cytokine productions were analyzed by ELISA using the culture supernatants from splenic T cell-stimulated plate-coated anti-CD3 mAb for 24 h. Results are shown as mean ± SD of triplicates and representative of four to five mice in each group. *B*, Proliferative response of splenic T cell-stimulated plate-coated anti-CD3 and CD28 mAbs from TCDD-treated mice was analyzed with CFSE dilutions during 72 h. Results are representative of three to five mice in each group. *C*, $Foxp3^+CD4^+$ Treg cells in spleen from TCDD-treated mice were analyzed by flow cytometry. Results are representative of three to five mice in each group. $Foxp3^+$ cells (%) are indicated as mean ± SD of three to five mice in each group. *, $p < 0.05$. *D*, T-bet and GATA-3 mRNA expressions of spleen from TCDD-treated mice were detected by real-time PCR. Data are shown as mean ± SD of four to six mice per each group. *, $p < 0.05$; **, $p < 0.005$. *E*, IL-17 production was analyzed by ELISA using the culture supernatants from splenic T cell-stimulated plate-coated anti-CD3 mAb for 24 h. Results are shown as mean ± SD of triplicates and representative of four mice in each group.

anti-CD28 mAbs, or LPS for 72 h, cell division of $CD4^+$ or $B220^+$-gated spleen cells was analyzed by flow cytometry.

ELISA

The JS-1-, SS-A/Ro-, SS-B/La-, or ss-DNA-specific Abs of sera from mice were measured by an ELISA reader (model 680; Bio-Rad) with a spectrophotometer reading at 490 nm. Igs (IgG2a and IgG1) in sera were determined by using the mouse immunoglobulins ELISA quantitation kit (Bethyl Laboratories). For detection of IL-2, IFN-γ, IL-4, IL-10, and IL-17 in the culture supernatants from anti-CD3 mAb-stimulated splenic $CD4^+$ T cells for 24 h, ELISA were performed by using each specific Ab for the cytokines as previously described (34).

Real-time quantitative RT-PCR

Total RNA was extracted from thymus, spleen, and cultured thymocytes in NFS/*sld* mice using Isogen (Wako Pure Chemical), and reverse transcribed. Transcript levels of T-bet, GATA-3, AhR, CYP1A1, Bcl-xL, TNF-α, IFN regulatory factor (IRF)-1, GADD45, IL-1β, autoimmune regulator (AIRE), salivary protein-1, GAD67, and β-actin were performed using DNA Engine OPTICOM system (Bio-Rad) with SYBR Premix Ex Tag (Takara Shuzo). Primer sequences were as follows: T-bet: forward, 5′-CCTGTTGTGGTCCAAGTTCAAC-3′ and reverse, 5′-CACAAACAT CCTGTAATGGCTTGT-3′; GATA-3: forward, 5′-GACTTGCCAGAAAG GCAGAC-3′, and reverse, 5′-AAAGAGGTCACCACCCACAG-3′; AhR: forward, 5′-ACATAACGGACGAAATCCTGACC-3′ and reverse, 5′-TC AACTCTGCACCTTGCTTAGGA-3′; CYP1A1: forward, 5′-CCATGACC GGGAACTGTGG-3′, and reverse, 5′-TCTGGTGAGCATCCTGGACA-3′; NF-κB: forward, 5′-ATGGCAGACGATGATCCCTA-3′ and reverse, 5′-TAGGCAAGGTCAGAATGCAC-3′; Bcl-xL: forward, 5′-AGAAGA AACTGAAGCAGAG-3′, and reverse, 5′-TCCGACTCACCAATACCT G-3′; TNF-α, forward, 5′-ATGAGCACAGAAAGCATGATC-3′, and reverse, 5′-AGATGATCTGAGTGTGAGGG-3′; GADD45: forward, 5′-TG GTGACGAACCCACATTCAT-3′, and reverse, 5′-ACCCACTGATCCAT GTAGCGAC-5′; IL-1β: forward, 5′-TGATGAGAATGACCTGTTCT-3′, and reverse, 5′-CTTCTTCAAAGATGAAGGAAA-3′; AIRE: forward, 5′-AAGGGAGCCCAGGTCACTAT-3′, and reverse, 5′-ATTGAGGAGGGA CTCCAGGT-3′; salivary protein-1: forward, 5′-GGCTCTGAAACTCA GGCAGA-3′, and reverse, 5′-TGCAAACTCATCCACGTTGT-3′; GAD67: forward, 5′-TGCAACCTCCTCGAACGCGG-3′, and reverse, 5′-CCAG GATCTGCTCCAGAGAC-3′; β-actin: forward, 5′-GTGGGCCGCTCT AGGCACCA-3′ and reverse, 5′-CGGTTGGCCTTAGGGTTCAG GGGGG-3′.

NF-κB transcription activity assay

The transcriptional activity of NF-κB of the nuclear extracts from thymocytes was analyzed with NF-κB transcription factor colorimetric assay kit (Millipore). Nuclear extracts were incubated with biotinylated double-strand oligonucleotide probe containing the consensus sequence for NF-κB on a streptavidin-coated plate. Captured complexes, including active NF-κB protein, were incubated with the primary Abs for p50 and RelA and HRP-conjugated secondary Ab and tetramethylbenzidine substrate. The absorbance of the samples was measured with microplate reader at 450 nm.

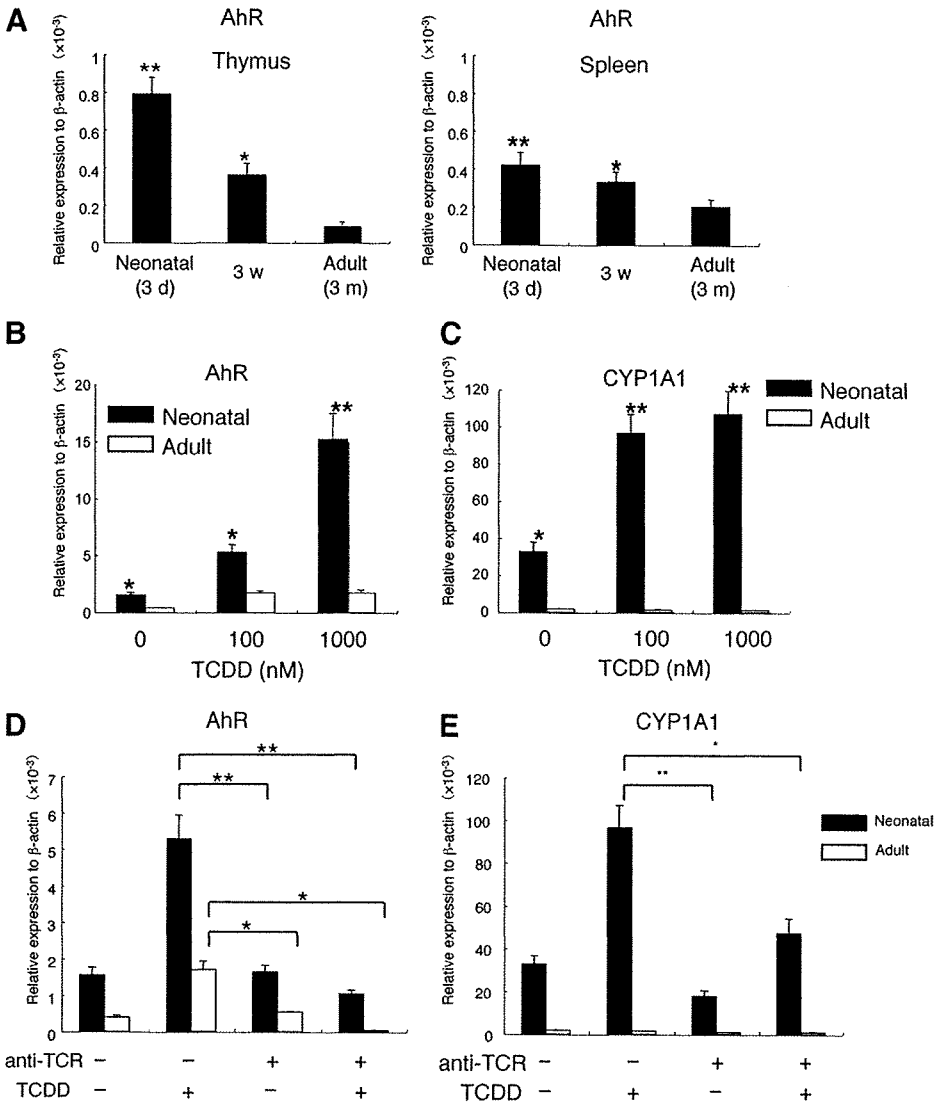

FIGURE 4. Cell signaling through AhR in thymus of NFS/*sld* mice. *A*, Expression of AhR mRNA of thymus and spleen from neonatal and adult NFS/*sld* mice was detected by quantitative RT-PCR. Relative expression to β-actin mRNA is indicated as mean ± SD of four mice in each group. *, $p < 0.05$; **, $p < 0.005$. w, Week. *B* and *C*, For 3 h in 24-well plate, 2×10^6 thymocytes of neonatal and adult NFS/*sld* mice were incubated with 0, 100, and 1000 nM TCDD. The mRNA expressions of AhR (*B*), and CYP1A1 (*C*) were analyzed by quantitative RT-PCR. *D* and *E*, The mRNA expressions of AhR (*D*) and CYP1A1 (*E*) in anti-TCR mAb-stimulated thymocytes from neonatal and adult mice with or without TCDD were detected by quantitative RT-PCR. Data are shown as mean ± SD of triplicate samples. *, $p < 0.05$; **, $p < 0.005$.

Statistical test

The Student *t* test was used for statistical analysis. Values of $p > 0.05$ were considered as significant.

Results

Induction of inflammatory lesions by neonatal administration of low-dose TCDD

To elucidate whether inflammatory lesions are induced by neonatal administration of low-dose TCDD into NFS/*sld* mice, i.p. injection of 0, 0.1, 1, and 10 ng/mouse TCDD was performed on day 0, 1, and 2 after birth. At 1, 2, and 6 mo of age, all the organs of treated mice were histopathologically analyzed. The inflammatory lesions in salivary glands of TCDD-injected mice, similar to those of thymectomized NFS/*sld* mice, were found whereas no lesion was observed in the salivary glands of vehicle-treated mice. The lesions of female mice were more severe than those of male mice (Fig. 1, *A–C*). Lymphocyte infiltration around ducts with destruction of acinar cells was observed in the TCDD-induced lesions (Fig. 1*A*). Severity of the inflammatory lesions was increased in a dose-dependent manner of TCDD (Fig. 1, *B* and *C*). In addition, more severe lesions developed with aging, and observed mainly in female mice (Fig. 1*C*). To characterize the infiltrating immune cells in the inflammatory lesions of salivary glands, the frozen sections were analyzed using the markers of T cells, B cells, and dendritic cells by immunofluorescence staining. $CD4^-$ T cells were mainly infiltrated in the inflammatory lesions of salivary glands from TCDD-treated mice, whereas a small population of $CD8^+$ T cells, B cells, and $CD11c^+$ dendritic cells were seen in the lesions (Fig. 1*D*).

In contrast, the inflammatory lesions of lung, liver, or kidney were also observed in the mice treated with TCDD (Fig. 1*E*). The incidence of the lesions is shown in Table I. At 6 mo of age, slight inflammatory lesions in the liver of 30–50% male mice by 0.1 or 1 ng of TCDD injection were observed. The inflammatory lesions of liver were found in 30–70% of male mice and ~50% of the female mice treated with 10 ng of TCDD at 6 mo of age. Also, the inflammatory lesions of lung with a small number of lymphocyte infiltrates around bronchus or blood vessels were observed in both 100% female and male mice treated with 10 ng of TCDD at 6 mo of age. In addition, the slight inflammation in the kidney from 100% male mice treated with 10 ng of TCDD was observed at 6 mo of age. As for female mice, the renal lesions were found in ~50% of the mice treated with 10 ng of TCDD at 6 mo of age. Induction of inflammatory lesions by TCDD might be dependent on the sex or the sensitivity of each organ, although its precise mechanism is unclear.

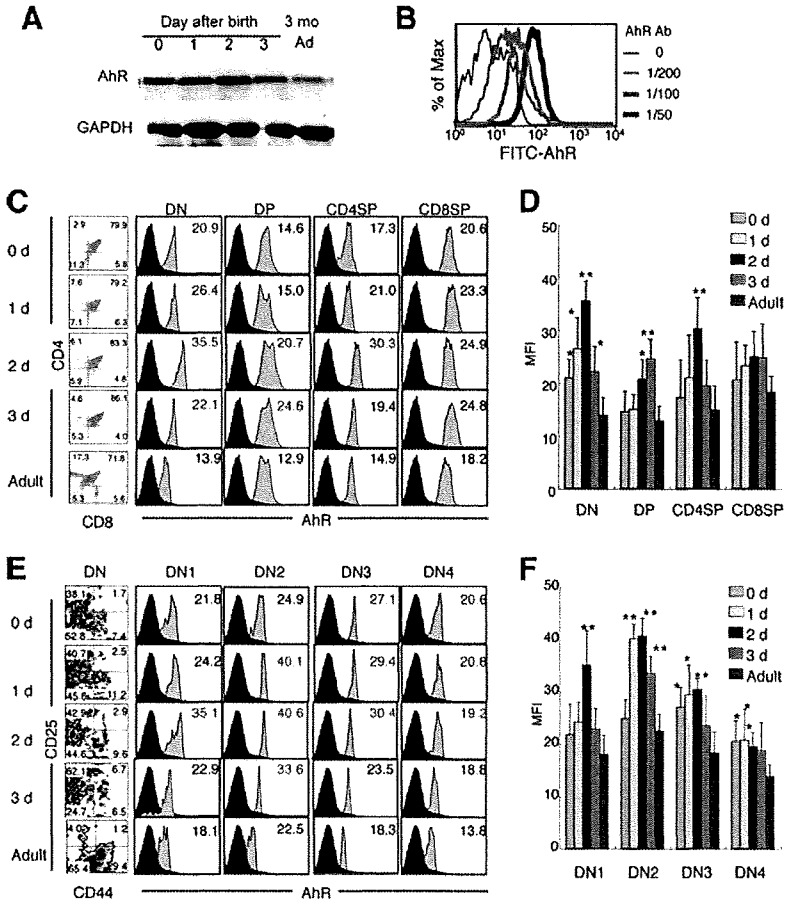

FIGURE 5. Expression of AhR in neonatal thymus. *A*, AhR protein of neonatal thymus from NFS/*sld* mice was detected by Western blotting. Result was representative of two independent experiments. GAPDH expression was used for loading control. *B*, Flow cytometric analysis of intracellular AhR expression. Thymocytes from B6 (3 mo) mice were stained with PE-Cy5.5-CD4 and PE-CD8 mAbs, fixed, washed in perm buffer, and then stained with rabbit anti-AhR Ab and FITC-conjugated anti-rabbit IgG as the second Ab. Diluted anti-AhR Ab (×200, ×100, and ×50) was used for staining. *C* and *D*, Thymocytes from neonatal (days 0, 1, 2, and 3 after birth) and adult (12 wk of age) NFS/*sld* mice were stained with PE-Cy5.5-CD4, PE-CD8, allophycocyanin-CD25, and PE-Cy7-CD44 mAbs, fixed, washed in permeabilization buffer, and then stained with rabbit anti-AhR Ab and FITC-conjugated anti-rabbit IgG as the second Ab. Intracellular AhR expressions of DN, DP, CD4SP, and CD8SP cells in neonatal and adult thymus. Figures are representative of three to four samples. Data are shown as mean ± SD of three to four samples. *E* and *F*, Intracellular AhR expression of DN cells in thymus. Data are shown as mean ± SD of mean fluorescence intensity (MFI) of three to four samples. Colored (blue or red) MFI was indicated in the figure as significantly increased. *, $p < 0.05$; **, $p < 0.005$.

Influence of in vivo low-dose TCDD injection on T cell phenotypes

To examine the influence of neonatal exposure to low-dose TCDD on T cell phenotypes, flow cytometric analysis of the expressions of surface T cell markers was performed on female mice at 6 mo of age (Fig. 2). There was no significant difference in the expression profile of CD4 and CD8 on the spleen cells by treatment of TCDD (Fig. 2*A*). A significantly increased population of memory phenotype, $CD44^{high}CD4^+$ T cell, was observed in the female mice treated with TCDD (Fig. 2*B*). As for thymic maturation, the $CD4^-CD8^-$ double-negative (DN) cells were considerably increased by treatment of 10 ng of TCDD while double-positive (DP) cells significantly decreased by 10 ng of TCDD injection. By contrast, both CD4 single-positive (SP) and CD8SP cells were significantly increased by TCDD injection (Fig. 2, *C* and *D*). Furthermore, when the increased DN cells were analyzed using differentiation markers such as CD25 and CD44, $CD44^+CD25^-$ (DN1) and $CD44^-CD25^-$ (DN4) cells were significantly reduced by in vivo treatment of 10 ng of TCDD, but significantly increased populations of $CD44^+CD25^+$ (DN2) and $CD44^-CD25^+$ (DN3) cells were observed (Fig. 2, *E* and *F*). These results suggested that neonatal exposure to TCDD might influence on thymic differentiation including negative or positive selection of T cells.

The influence of low-dose TCDD on peripheral T cell functions

To know the effect of TCDD on T cell functions in the periphery, cytokine secretions from splenic T cells activated by plate-coated anti-CD3 mAb were analyzed using the culture supernatants by ELISA. T_H1 cytokine production, including IL-2 and IFN-γ from activated T cells of TCDD-treated mice, was significantly increased compared with that of control mice (Fig. 3*A*). By contrast, there was no influence on T_H2 cytokine secretion such as IL-4 and IL-10 by in vivo TCDD injection (Fig. 3*A*). Moreover, proliferative response of splenic T cells stimulated with anti-CD3 and CD28 mAbs was analyzed using CFSE dilutions during 3 days. The cell divisions during the late stage were significantly enhanced by in vivo TCDD injection compared with those of control mice (Fig. 3*B*). In contrast, there was no difference in $Foxp3^+$ $CD25^+CD4^+$ T cells, classical Treg cells, by neonatal TCDD exposure (Fig. 3*C*). It has been known that T-bet for T_H1 and GATA-3 for T_H2 are prime candidates for key transcription factors of each cytokine production of T_H cells (35). T-bet mRNA expression of purified T cells from spleen in TCDD-treated mice was higher than that in control mice. However, there was no change of the GATA-3 mRNA expression by TCDD injection (Fig. 3*D*). In addition, to examine the role of IL-17 in the pathogenesis for TCDD-induced autoimmunity, no change was observed in IL-17 production from anti-CD3 mAb-stimulated T cells of TCDD-treated mice (Fig. 3*E*). These findings show that the neonatal exposure to low-dose TCDD influences on T cell activation or proliferation through enhanced secretion of T_H1 cytokines in the periphery.

Direct influences of TCDD on neonatal thymus

When adult NFS/*sld* mice at 2 mo of age were injected with low-dose TCDD, no inflammatory lesion in any organ was observed until 6 mo of age (our unpublished data). Neonatal exposure to low-dose TCDD may affect the induction of inflammatory lesions in salivary glands resembling the SS model. To evaluate whether

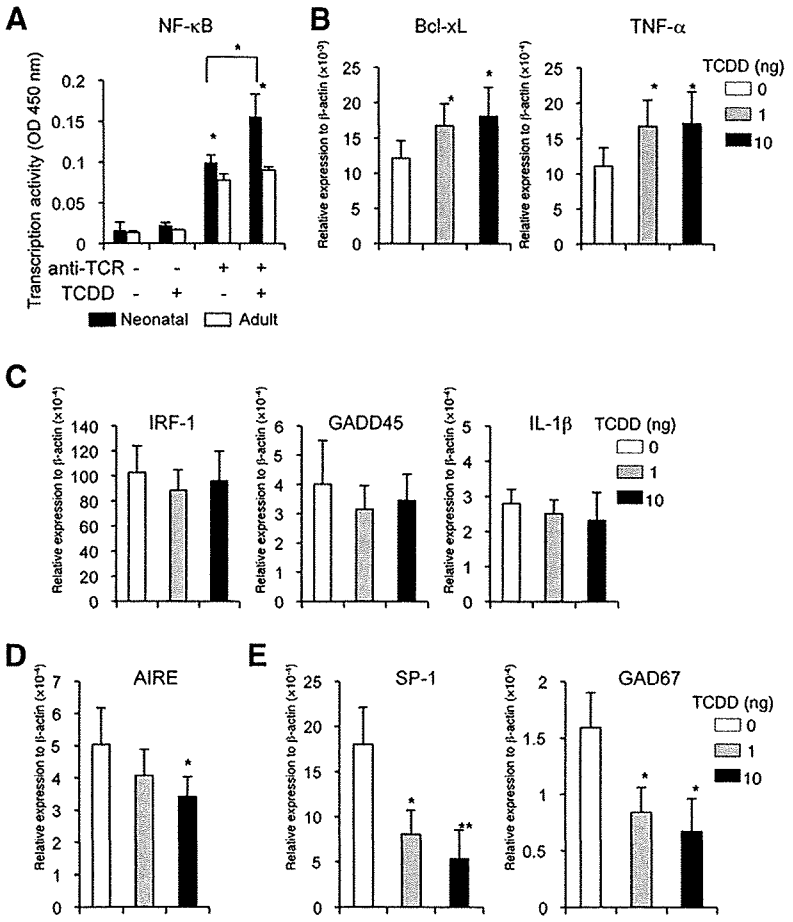

FIGURE 6. Influence of TCDD on central tolerance in thymus. *A*, Transcription activity of NF-κB in thymocytes stimulated with anti-TCR mAb in the presence or absence of TCDD was evaluated. Results are shown as mean ± SD of three samples. *, $p < 0.05$. *B* and *C*, In vivo effect of TCDD on target genes of NF-κB was evaluated to detect the mRNA expressions. The mRNA expressions of NF-κB-regulated genes in thymus tissues from TCDD-treated mice were analyzed by real time-PCR. Results are shown as mean ± SD of four to six mice per each group. *, $p < 0.05$. *D*, AIRE mRNA expression of thymus from TCDD-treated mice. *E*, The mRNA expressions of salivary protein-1 and GAD67 in thymus from TCDD-treated mice. The expressions of thymus from TCDD-treated mice were detected by real-time PCR. *, $p < 0.05$; **, $p < 0.005$.

the exposure to TCDD has much more influence on neonatal thymus compared with adult thymus, the expression of AhR was analyzed by quantitative RT-PCR. Interestingly, in contrast to adult thymus, the expression of AhR mRNA of neonatal thymus from NFS/*sld* mice was much higher (8- to 9-fold) (Fig. 4*A*). The expression was reduced with aging (~3 mo of age). The expression of AhR mRNA in neonatal spleen was higher (2-fold) than that in adult spleen (Fig. 4*A*). Next, to clarify the direct effects of TCDD on thymocytes, neonatal and adult thymocytes were incubated with 0, 100, and 1000 nM TCDD for 3 h to analyze AhR expression. More increased expression of AhR in neonatal thymocytes was observed by TCDD stimulation compared with that in adult thymocytes (Fig. 4*B*). In addition, mRNA expression of CYP1A1, one of target genes for TCDD/AhR/XRE (36), in neonatal thymocytes was much enhanced by TCDD incubation, whereas there was no change in mRNA expression of CYP1A1 in adult thymocytes by TCDD stimulation (Fig. 4*C*). In contrast, there were no significant changes in mRNA expressions of AhR and CYP1A1 of the spleen cells in the response to TCDD between neonatal and adult mice (data not shown). To understand association between TCR and TCDD signaling in thymocytes of neonatal and adult NFS/*sld* mice, plate-coated anti-TCRβ mAb was used for the stimulation of thymocytes with or without TCDD. Up-regulated mRNA expression of AhR by TCDD in both neonatal and adult thymocytes was clearly reduced by stimulation of anti-TCRβ mAb (Fig. 4*D*). In addition, TCDD-induced CYP1A1 mRNA expression in neonatal thymocytes was reduced to the level of non-stimulation by anti-TCRβ mAb (Fig. 4*E*). These findings suggest that neonatal thymocytes may be sensitive to TCDD through highly expressed AhR in NFS/*sld* mice, and that neonatal injection of TCDD might influence thymic differentiation to induce breakdown of tolerance.

Expression of AhR in neonatal thymus

To confirm the higher expression of AhR as a protein in neonatal thymus tissues of NFS/*sld* mice, Western blot analysis was performed. The highest expression of AhR was observed on day 2 after birth, and the expression on day 3 was relatively decreased. The expression in adult (3 mo of age) was lower than that of neonatal thymus (Fig. 5*A*). Next, we tried to detect the intracellular AhR expression in subpopulation of thymocytes by flow cytometric analysis. Flow cytometric analysis showed that most thymocytes clearly expressed AhR in adult (3 mo of age) C57BL/6 mice, and the fluorescence intensity of AhR expression was increased depending on the dose of anti-AhR Ab (Fig. 5*B*). When compared, the AhR expressions at each stage including DN, DP, CD4SP, and CD8SP cells in neonatal thymus of NFS/*sld* mice from day 0 to day 3 after birth with those in adult thymus (3 mo), a significantly increased AhR expression of neonatal (days 0, 1, 2, and 3) DN T cells was observed than that of adult DN cells. In particular, much more AhR expression of DN cells on day 2 was detected during neonatal stage. AhR expression of DP T cells on days 2 and 3 was significantly higher than that of adult DP cells. In contrast, although AhR expression of CD4SP cells on day 2 was significantly higher than that of adult CD4SP cells, there was no change in the expression of AhR of CD8SP cells between neonatal and adult thymus (Fig. 5, *C* and *D*). Furthermore, when the AhR expression of each differentiation stage of DN such as $CD44^+CD25^-$ (DN1), $CD44^+CD25^+$ (DN2), $CD44^-CD25^+$ (DN3), and $CD44^-CD25^-$

(DN4) cells was analyzed, AhR expressions of DN1 cells on day 2, DN2 cells on days 1, 2, and 3, DN3 cells on days 0, 1, and 2, and DN4 cells on days 0, 1, and 2 were significantly higher than those of adult DN cells (Fig. 5, *E* and *F*). Among them, the expressions of neonatal DN2 and DN3 cells were more intensive compared with those of adult thymocytes. In contrast, there was no difference in AhR expression at each stage between neonatal and adult thymocytes from normal B6 mice (data not shown). These findings suggest that AhR expression may be related with development and differentiation of T cells in neonatal thymus of NFS/*sld* mice, and that sensitivity of TCDD in neonates can be explained by the development of autoimmunity through AhR expression.

The influence of exposure to low-dose TCDD on central tolerance

Because higher AhR expression of T cells in neonatal thymus of NFS/*sld* mice was observed (Fig. 5), the cell signal pathway to regulate central tolerance in thymus via TCDD/AhR was analyzed. We focused on NF-κB, one of the responsive factors for TCDD/AhR/XRE signaling (37), which is known to be a key transcription factor for regulation of T cell differentiation, development, and activation (38). When the transcriptional activity of NF-κB in between neonatal and adult thymocytes stimulated with anti-TCR mAb in the presence of TCDD was compared, the neonatal activity was significantly increased relative to that of adult thymocytes (Fig. 6*A*). Also, the NF-κB activity of neonatal thymocytes stimulated with anti-TCR mAb was largely enhanced by the addition of TCDD, whereas the increased activity of adult thymocytes was not observed (Fig. 6*A*). Next, to understand the in vivo cell signaling through NF-κB and TCDD/AhR in thymus, the mRNA levels of NF-κB target genes were analyzed by real-time PCR using the thymus tissues from neonatal TCDD-treated mice. Among them, Bcl-xL and TNF-α mRNAs in thymus tissues from TCDD-treated mice were significantly increased in the dose-dependent manner compared with control mice (Fig. 6*B*). There were no changes to the mRNA expressions of IRF-1, GADD45, IL-1β (Fig. 6*C*), IL-6, inducible NO synthase, and Fas ligand (data not shown) which are target genes of NF-κB for controlling T cell signal.

In contrast, AIRE, an essential transcription factor for the expression of tissue-specific autoantigen in thymic epithelial cells (TECs), is well known to play a key role in T cell differentiation and development related with autoimmunity (39). When AIRE mRNA level in thymus tissues, including TECs from neonatal TCDD-treated NFS/*sld* mice, was analyzed, the expression in 10 ng of TCDD-treated mice was significantly decreased compared with that in control mice (Fig. 6*D*). Moreover, salivary protein-1 and GAD67 are known to be representative for the tissue-specific Ag in salivary gland and pancreas respectively (40). Interestingly, both salivary protein-1 and GAD67 mRNA expressions of the thymus tissues from neonatal TCDD-treated NFS/*sld* mice were significantly reduced relative to those from control mice (Fig. 6*E*). These findings show that neonatal exposure to low-dose TCDD in NFS/*sld* mice might influence the impairment of central tolerance in thymus, resulting in the induction of autoimmune disease.

The influences of low-dose TCDD exposure on B cells

The effects of neonatal exposure to low-dose TCDD on B cell phenotype and function were analyzed (Fig. 7). There was no difference in the number of $B220^+$ B cells from spleen between TCDD-treated and control mice (Fig. 7*A*). Furthermore, no change was observed in the proliferative response of splenic B cells to LPS from TCDD-treated mice compared with that from control mice (Fig. 7*B*). The serum titers of autoantibodies that are associated with SS, including anti-SSA/Ro, anti-SSB/La, and anti-ssDNA, were examined (17, 18). In this study, serum titers of anti-SSA/Ro and anti-SSB/La autoantibodies were significantly increased in TCDD-treated mice at 6 mo of age compared with those in control mice (Fig. 7*C*). It has been reported that thymectomized NFS/*sld* mice and human SS patients have high titers of serum autoantibody against α-fodrin (20, 34). The higher titers of anti-α-fodrin autoantibody in the sera from TCDD-treated mice were also detected from control mice at 6 mo of age (Fig. 7*D*). No significant change for anti-ssDNA was observed between TCDD-treated and control mice (data not shown). In addition, when the ratio of IgG2a and IgG1 that is associated with T_H1 and T_H2 or cellular and humoral immune responses was analyzed using sera from TCDD-injected mice, the ratio from TCDD-injected mice was significantly higher than that from control mice at 6 mo of age (Fig. 7*E*).

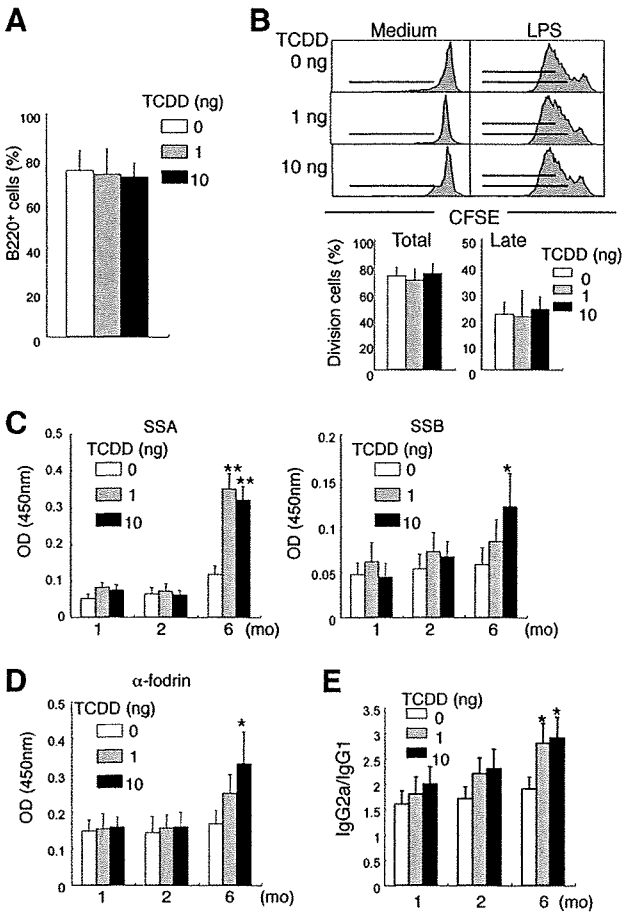

FIGURE 7. Influence on B cell functions by neonatal exposure to low-dose TCDD. *A*, $B220^-$ B cells in spleen from TCDD-treated mice at 6 mo of age were detected by flow cytometric analysis. Results are shown as mean ± SD of five to seven mice in each group. *B*, Proliferative response of splenic B cells stimulated with LPS was evaluated with CFSE dilutions during 72 h. Figures are representative of five to seven mice in each group. *C* and *D*, Serum titers of autoantibodies, including anti-SSA/Ro, anti-SSB/Lo, and anti-α-fodrin from female TCDD-treated mice from 1 to 6 mo of age were measured by ELISA. Results are shown as mean ± SD of five to seven mice in each group. *E*, Ratio of IgG2a/IgG1 in sera from TCDD-injected mice. Serum titer of IgG2a and IgG1 from TCDD-injected NFS/*sld* mice was measured by ELISA. Data are shown as mean ± SD of the ratio from five to seven mice. *, $p < 0.05$; **, $p < 0.005$.

Discussion

TCDD is a widespread environmental contaminant that influences several basic homeostatic control mechanisms in the body via AhR (3). T cells are a possible direct target for TCDD, as evidenced by the presence of the AhR in T cells, and inhibition of T cell growth by the expression of a constitutively active AhR mutant in AhR-null Jurkat T cells or following TCDD treatment (1, 41). It has been demonstrated that expression of AhR in both $CD4^+$ and $CD8^+$ T cells is required for a full suppression of an allospecific CTL response by TCDD, indicating a direct role for AhR in these TCDD-induced immunosuppressive effects (1, 42). However, the relationship between in vivo TCDD exposure and breakdown in T cell tolerance has not been well defined.

In this study, we demonstrated that neonatal exposure to low-dose TCDD could induce autoimmunity in the salivary glands using a NFS/*sld* strain associated with disease-susceptible autoantibody production, such as anti-SSA/La, anti-SSB/Ro, and anti-α-fodrin Abs. It has been reported that TCDD causes extensive damage to the thymus to suppress T cell-dependent immune responses in vivo, including delayed-type and contact hypersensitivity responses and the generation of CTL (4, 43, 44). By contrast, neonatal exposure to TCDD had little influence on thymic atrophy in our experiment in which low-dose (0.0486 ± 0.0088 to 8.37 ± 0.7 μg/kg) TCDD was administered into neonatal mice on days 0, 1, and 2 (body weight: 1.2 ± 0.1 to 2.1 ± 0.35 g) after birth. The dosage of TCDD was considerably lower than that in the experiments in which thymic atrophy or apoptosis was induced by in vivo exposure to TCDD (30–50 μg/kg) (31, 32). For instance, it was reported that 60% apoptotic cells of thymus were observed in normal mice injected with 50 μg/kg TCDD, whereas 20–30% apoptotic cells of thymus were observed in vehicle-injected mice. In addition, although the loss of mitochondrial membrane potential related to apoptosis of thymocytes was not detected in ~10 μg/kg TCDD-treated mice, the loss was observed in 10–50 μg/kg TCDD-treated mice (31). Thus, the exposure to low dosage under 10 μg/kg TCDD may have an influence on neonatal thymic differentiation or selection in NFS/*sld* mice, but not atrophy or apoptosis, to induce autoimmune disease as the late effect. Moreover, T cell proliferation by anti-CD3 and -CD28 mAbs and Th1-type cytokine production, such as IL-2 and IFN-γ from splenic $CD4^+$ T cells, were significantly more enhanced by neonatal TCDD treatment than those in control mice. These findings were consistent with the reports that TCDD enhances proliferation and cytokine production of mitogen- or Ag-stimulated T cells or T cell clones (1, 8). Because there were alterations in the percentage and number of DN cells in TCDD-treated mice, we analyzed this population using CD44 and CD25 markers. After TCDD treatment in this set, there was a decrease in the percentage of $CD44^+CD25^-$ cells (DN1) and $CD44^-CD25^-$ cells (DN4), and a relative increase in the percentage of $CD44^+CD25^+$ cells (DN2) and $CD44^-CD25^+$ cells (DN3). Analysis of the actual numbers of cells in each population compared with controls suggested that thymic maturation or negative selection at DN2 or DN3 might be affected by neonatal exposure to the low-dose TCDD. These results suggest that TCDD is interfering with the development and/or the proliferation of DN cells. Furthermore, the early stage of DN and the late stage into CD4SP or CD8SP in the thymic differentiation were disturbed by low-dose TCDD treatment, indicating that the immunotoxicity of TCDD on neonatal thymus might lead to the development of T cell-dependent autoimmunity. The inflammatory lesions were observed in the organs other than salivary gland including kidney, lung, and liver in TCDD-treated mice. Although the inflammatory lesions in liver, lung, and kidney from female mice treated with 10 ng of TCDD at 2 mo of age were observed, the severity of extraglandular lesions was lower than that of salivary gland, and the onset was later compared with that in salivary gland. Most of the extraglandular lesions of both female and male mice were developed with aging. We have previously demonstrated that the extraglandular lesion such as autoimmune arthritis in 3d-Tx NFS/*sld* mice was observed with aging (45, 46). Therefore, it is possible that TCDD may enhance any age-related reaction in the organs to induce autoimmunity.

In this study, there were no changes in the B cell number and proliferation in spleen from low-dose TCDD-treated mice, although the suppressive effect of the T cell-dependent Ab response to sheep RBC was reported in C57BL/6 mice injected with TCDD (47). In addition, TCDD selectively inhibited terminal B cell differentiation into plasma cells in response to trinitrophenol-LPS without altering early events in B cell activation or proliferation (48). By contrast, in our study significantly increased autoantibody productions such as anti-SSA/La, anti-SSB/Ro, and anti-α-fodrin were observed by neonatal exposure to low-dose TCDD. Although it is still unclear whether the direct or indirect effect of TCDD on B cells influences autoantibody production, this new finding may be a key to understand the association of TCDD immunotoxicity with the development of autoimmunity.

AhR is a cytoplasmic receptor protein and has been described as a ligand-activated transcription factor that mediates induction of xenobiotic metabolizing enzymes (27, 28, 49). Upon ligand binding, the AhR translocates into the nucleus and dimerizes with ARNT. The AhR/ARNT complex binds to specific gene promoter elements (50). In this study, significantly increased expressions of AhR mRNA and protein in neonatal thymus were observed compared with those in adult thymus. This suggests that neonatal exposure to low-dose TCDD may effect thymic differentiation and/or maturation through AhR by disrupting the T cell tolerance more intensively than those in adult thymus. If negative or positive selection in the neonatal thymus is disrupted by low-dose TCDD exposure, autoreactive T cells may be released to the periphery and expand in response to any autoantigen leading to induce autoimmunity. Increased expression of AhR mRNA and the disrupted thymic differentiation in the neonatal thymus by low-dose TCDD exposure may support this hypothesis.

CYP1A1 is known to have pivotal roles in cell growth and apoptosis (51, 52). In the present study, CYP1A1 mRNA of neonatal thymocytes was readily up-regulated by TCDD, whereas the expression of adult thymocytes was constant in the response to TCDD. Neonatal exposure to low-dose TCDD may influence proliferation, differentiation, or apoptosis of thymocytes through CYP1A1 at early stages, such as DN. Namely, it is possible that negative selection leading cell apoptosis at DN3 might be disturbed by neonatal exposure to TCDD. As a result, autoreactive T cells leaking from thymic selection might survive and proliferate in response to any autoantigen in the periphery, leading to the induction of autoimmune lesions. The activation of AhR by TCDD results in an increased binding activity to NF-κB subunit RelB of AhR itself to form AhR/RelB complex, which was associated with an increased mRNA level of multiple inflammatory genes (53). Overexpression of AhR and RelB led to an increased level of CCL1 and IRF-3 in control as well as TCDD-stimulated cells supporting the role of RelB and AhR for the transcriptional regulation of these genes (54). In the present study, TCDD enhanced TCR-mediated classical NF-κB activation of neonatal thymocytes from NFS/*sld* mice more than adult thymocytes. In addition, some NF-κB-target genes such as Bcl-x_L and TNF-α in thymus were up-regulated by in vivo TCDD injection. Our data demonstrate that

TCDD/AhR signal may influence the differentiation or development of T cells in the neonatal thymus associated with autoimmunity. However, the precise mechanism of how the NF-κB activation, including classical and nonclassical pathway, interacts with TCDD/AhR signal is still unclear.

It has been well known that autoimmune lesions of multiple organs such as lacrimal glands, salivary glands, pancreas, and liver are observed in AIRE gene-deficient mice (39). AIRE was reported to play a pivotal role in the expression of tissue-specific autoantigens such as salivary protein-1, GAD67, insulin, or other self-proteins in the TECs that express the MHC class II on the cell surface and function as APCs to immature T cells for the immunological selection of central tolerance in the thymus (55). In this study, mRNA expressions of AIRE and tissue-specific autoantigens such as salivary protein-1 and GAD67 in the thymus were reduced by the in vivo neonatal exposure to low-dose TCDD in NFS/*sld* mice. The finding indicated that TCDD might influence the selection of autoreactive T cells in the thymus through AIRE. There may be any complex molecular mechanisms related to the avidity of TCR, haplotype of MHC class II, Ag-specificity, T cell apoptosis, interaction with TEC, or TCDD signal.

The AhR has been shown to mediate various immunotoxic responses induced by environmental pollutants like TCDD (56). Although our results show that activation of the AhR by TCDD effects T cell development, the receptor does not seem to play a key role in the establishment of a normal T cell compartment. The AhR has been shown to play important roles in regulating the expression of several cytokines. For example, exposure of rats to TCDD led to up-regulation of IL-1β and TNF-α in the liver (57, 58). Interestingly, although TCDD suppressed the production of IFN-γ by mediastinal lymph node cells, there was a 10-fold increase in the IFN-γ level in the lungs of TCDD-treated mice (59). Autoimmune disease is caused by heterogeneous etiology, involving interplay between predisposing genes and triggering environmental factors. Although a lot of studies have demonstrated the immunotoxicity of TCDD, this study is the first to induce autoimmunity by neonatal low-dose TCDD treatment. Recently it has been reported that AhR links T_H17 cell-mediated experimental autoimmune encephalomyelitis to environmental toxins through altering the differentiation of Treg cells (60, 61). The low-dose TCDD exposure in our model had little influence on the number of Treg cells in spleen and the function of T_H17 cells, such as IL-17 production from T cells. The action of TCDD via AhR may influence peripheral tolerance related to autoimmunity besides central tolerance in thymus.

Taken together, our new findings may explain the risk for autoimmunity caused by the late effect of early exposure to environmental pollution, including TCDD. And as shown here, our model would help to understand the multifactorial nature of autoimmune disease.

Acknowledgments

We thank Ai Nagaoka, Noriko Kino, Risa Okada, Ritsuko Oura, and Satoko Yoshida for technical assistance.

Disclosures

The authors have no financial conflict of interest.

References

1. Kerkvliet, N. I. 2001. Recent advances in understanding the mechanisms of TCDD immunotoxicity. *Int. Immunopharmacol.* 2: 277–291.
2. Wormley, D. D., A. Ramesh, and D. B. Hood. 2004. Environmental contaminant-mixture effects on CNS development, plasticity, and behavior. *Toxicol. Appl. Pharmacol.* 197: 49–65.
3. Schecter, A., L. Birnbaum, J. J. Ryan, and J. D. Constable. 2006. Dioxins: an overview. *Environ. Res.* 101: 419–428.
4. Laiosa, M. D., A. Wyman, F. G. Murante, N. C. Fiore, J. E. Staples, T. A. Gasiewicz, and A. E. Silverstone. 2003. Cell proliferation arrest within intrathymic lymphocyte progenitor cells causes thymic atrophy mediated by the aryl hydrocarbon receptor. *J. Immunol.* 171: 4582–4591.
5. Gehrs, B. C., and R. J. Smialowicz. 1999. Persistent suppression of delayed-type hypersensitivity in adult F344 rats after perinatal exposure to 2,3,7,8-tetrachlorodibenzo-p-dioxin. *Toxicology* 134: 79–88.
6. Walker, D. B., W. C. Williams, C. B. Copeland, and R. J. Smialowicz. 2004. Persistent suppression of contact hypersensitivity, and altered T-cell parameters in F344 rats exposed perinatally to 2,3,7,8-tetrachlorodibenzo-*p*-dioxin (TCDD). *Toxicology* 197: 57–66.
7. Prell, R. A., E. Dearstyne, L. G. Steppan, A. T. Vella, and N. I. Kerkvliet. 2000. CTL hyporesponsiveness induced by 2,3,7,8-tetrachlorodibenzo-*p*-dioxin: role of cytokines and apoptosis. *Toxicol. Appl. Pharmacol.* 166: 214–221.
8. Prell, R. A., J. A. Oughton, and N. I. Kerkvliet. 1995. Effect of 2,3,7,8-tetrachlorodibenzo-*p*-dioxin on anti-CD3-induced changes in T-cell subsets and cytokine production. *Int. J. Immunopharmacol.* 17: 951–961.
9. Shepherd, D. M., E. A. Dearstyne, and N. I. Kerkvliet. 2000. The effects of TCDD on the activation of ovalbumin (OVA)-specific DO11.10 transgenic CD4(+) T cells in adoptively transferred mice. *Toxicol. Sci.* 56: 340–350.
10. Morris, D. L., J. G. Karras, and M. P. Holsapple. 1993. Direct effects of 2,3,7,8-tetrachlorodibenzo-p-dioxin (TCDD) on responses to lipopolysaccharide (LPS) by isolated murine B-cells. *Immunopharmacology* 26: 105–112.
11. Karras, J. G., and M. P. Holsapple. 1994. Inhibition of calcium-dependent B cell activation by 2,3,7,8-tetrachlorodibenzo-*p*-dioxin. *Toxicol. Appl. Pharmacol.* 125: 264–270.
12. Dooley, R. K., D. L. Morris, and M. P. Holsapple. 1990. Elucidation of cellular targets responsible for tetrachlorodibenzo-p-dioxin (TCDD)-induced suppression of antibody responses. II. The role of the T-lymphocyte. *Immunopharmacology* 19: 47–58.
13. Gotter, J., and B. Kyewski. 2004. Regulating self-tolerance by deregulating gene expression. *Curr. Opin. Immunol.* 16: 741–745.
14. Anderton, S., C. Burkhart, B. Metzler, and D. Wraith. 1999. Mechanisms of central and peripheral T-cell tolerance: lessons from experimental models of multiple sclerosis. *Immunol. Rev.* 169: 123–127.
15. Miller, J. F., and R. A. Flavell. 1994. T-cell tolerance and autoimmunity in transgenic models of central and peripheral tolerance. *Curr. Opin. Immunol.* 6: 892–899.
16. Kruize, A. A., R. J. Sweenk, and L. Kater. 1995. Diagnostic criteria and immunopathogenesis of Sjögren's syndrome: implications for therapy. *Immunol. Today* 16: 557–559.
17. Fox, R. I., M. Stern, and P. Michelson. 2000. Update in Sjögren syndrome. *Curr. Opin. Rheumatol.* 12: 391–398.
18. Fox, R. I. 2005. Sjögren's syndrome. *Lancet* 366: 321–331.
19. Haneji, N., H. Hamano, K. Yanagi, and Y. Hayashi. 1994. A new animal model for primary Sjögren's syndrome in NFS/*sld* mutant mice. *J. Immunol.* 153: 2769–2777.
20. Haneji, N., T. Nakamura, K. Takio, K. Yanagi, H. Higashiyama, I. Saito, S. Noji, H. Sugino, and Y. Hayashi. 1997. Identification of α-fodrin as a candidate autoantigen in primary Sjögren's syndrome. *Science* 275: 604–607.
21. Saegusa, K., N. Ishimaru, K. Yanagi, K. Mishima, R. Arakaki, T. Suda, I. Saito, and Y. Hayashi. 2002. Prevention and induction of autoimmune exocrinopathy is dependent on pathogenic autoantigen cleavage in murine Sjögren's syndrome. *J. Immunol.* 169: 1050–1057.
22. Suri-Payer, E., K. Wei, and K. Tung. 2001. The day-3 thymectomy model for induction of multiple organ-specific autoimmune diseases. *Curr. Protoc. Immunol.* 15: 15–16.
23. Kojima, A., Y. Tanaka-Kojima, T. Sakakura, and Y. Nishizuka. 1976. Spontaneous development of autoimmune thyroiditis in neonatally thymectomized mice. *Lab. Invest.* 34: 550–557.
24. Teague, P. O., E. J. Yunis, G. Rodey, A. J. Fish, O. Stutman, and R. A. Good. 1970. Autoimmune phenomena and renal disease in mice: role of thymectomy, aging, and involution of immunologic capacity. *Lab. Invest.* 22: 121–130.
25. Tung, K. S., S. Smith, P. Matzner, K. Kasai, J. Oliver, F. Feuchter, and R. E. Anderson. 1987. Murine autoimmune oophoritis, epididymoorchitis, and gastritis induced by day 3 thymectomy. *Am. J. Pathol.* 126: 303–314.
26. Safe, S. 2001. Molecular biology of the Ah receptor and its role in carcinogenesis. *Toxicol. Lett.* 120: 1–7.
27. Denison, M. S., and S. Heath-Pagliuso. 1998. The Ah receptor: a regulator of the biochemical and toxicological actions of structurally diverse chemicals. *Bull. Environ. Contam. Toxicol.* 61: 557–568.
28. Marlowe, J. L., and A. Puga. 2005. Aryl hydrocarbon receptor, cell cycle regulation, toxicity, and tumorigenesis. *J. Cell. Biochem.* 96: 1174–1184.
29. Nohara, K., H. Fujimaki, S. Tsukumo, K. Inouye, H. Sone, and C. Tohyama. 2002. Effects of 2,3,7,8-tetrachlorodibenzo-*p*-dioxin (TCDD) on T cell-derived cytokine production in ovalbumin (OVA)-immunized C57Bl/6 mice. *Toxicology* 172: 49–58.
30. Neff-LaFord, H. D., B. A. Vorderstrasse, and B. P. Lawrence. 2003. Fewer CTL, not enhanced NK cells, are sufficient for viral clearance from the lungs of immunocompromised mice. *Cell. Immunol.* 226: 54–64.
31. Tomita, S., H. B. Jiang, T. Ueno, S. Takagi, K. Tohi, S. Mackawa, A. Miyatake, A. Furukawa, F. J. Gonzalez, J. Takeda, T. Ichikawa, and Y. Takahama. 2003. T cell-specific disruption of arylhydrocarbon receptor nuclear translocator (Arnt) gene causes resistance to 2,3,7,8-tetrachlorodibenzo-*p*-dioxin-induced thymic involution. *J. Immunol.* 171: 4113–4120.
32. Camacho, I. A., N. Singh, V. L. Hegde, M. Nagarkatti, and P. S. Nagarkatti. 2005. Treatment of mice with 2,3,7,8-tetrachlorodibenzo-*p*-dioxin leads to aryl

hydrocarbon receptor-dependent nuclear translocation of NF-κB and expression of Fas ligand in thymic stromal cells and consequent apoptosis in T cells. *J. Immunol.* 175: 90–103.
33. White, S. C., and G. W. Casarett. 1974. Induction of experimental autoallergic sialadenitis. *J. Immunol.* 112: 178–185.
34. Kohashi, M., N. Ishimaru, R. Arakaki, and Y. Hayashi. 2008. Effective treatment with oral administration of rebamipide in a mouse model for Sjogren's syndrome. *Arthritis Rheum.* 58: 389–400.
35. Rengarajan, J., S. J. Szabo, and L. H. Glimcher. 2000. Transcriptional regulation of Th1/Th2 polarization. *Immunol. Today* 21: 479–783.
36. Riddick, D. S., Y. Huang, P. A. Harper, and A. B. Okey. 1994. 2,3,7,8-Tetrachlorodibenzo-*p*-dioxin versus 3-methylcholanthrene: comparative studies of Ah receptor binding, transformation, and induction of CYP1A1. *J. Biol. Chem.* 269: 12118–12128.
37. Singh, N. P., M. Nagarkatti, and P. S. Nagarkatti. 2007. Role of dioxin response element and nuclear factor-κB motifs in 2,3,7,8-tetrachlorodibenzo-*p*-dioxin-mediated regulation of Fas and Fas ligand expression. *Mol. Pharmacol.* 71: 145–157.
38. Bonizzi, G., and M. Karin. 2004. The two NF-κB activation pathways and their role in innate and adaptive immunity. *Trends Immunol.* 25: 280–288.
39. Anderson, M. S., E. S. Venanzi, L. Klein, Z. Chen, S. P. Berzins, S. J. Turley, H. von Boehmer, R. Bronson, A. Dierich, C. Benoist, and D. Mathis. 2002. Protection of an immunological self shadow within the thymus by the aire protein. *Science* 298: 1395–1401.
40. Kuroda, N., T. Mitani, N. Takeda, N. Ishimaru, R. Arakaki, Y. Hayashi, Y. Bando, K. Izumi, T. Takahashi, T. Nomura, et al. 2005. Development of autoimmunity against transcriptionally unrepressed target antigen in the thymus of Aire-deficient mice. *J. Immunol.* 174: 1862–1870.
41. Ito, T., S. Tsukumo, N. Suzuki, H. Motohashi, M. Yamamoto, Y. Fujii-Kuriyama, J. Mimura, T. M. Lin, R. E. Peterson, C. Tohyama, and K. Nohara. 2004. A constitutively active arylhydrocarbon receptor induces growth inhibition of Jurkat T cells through changes in the expression of genes related to apoptosis and cell cycle arrest. *J. Biol. Chem.* 279: 25204–25210.
42. Nagarkatti, P. S., G. D. Sweeney, J. Gauldie, and D. A. Clark. 1984. Sensitivity to suppression of cytotoxic T cell generation by 2,3,7,8-tetrachlorodibenzo-*p*-dioxin (TCDD) is dependent on the Ah genotype of the murine host. *Toxicol. Appl. Pharmacol.* 72: 169–176.
43. Nohara, K., X. Pan, S. Tsukumo, A. Hida, T. Ito, H. Nagai, K. Inouye, H. Motohashi, M. Yamamoto, Y. Fujii-Kuriyama, and C. Tohyama. 2005. Constitutively active aryl hydrocarbon receptor expressed specifically in T-lineage cells causes thymus involution and suppresses the immunization-induced increase in splenocytes. *J. Immunol.* 174: 2770–2777.
44. Staples, J. E., F. G. Murante, N. C. Fiore, T. A. Gasiewicz, and A. E. Silverstone. 1998. Thymic alterations induced by 2,3,7,8-tetrachlorodibenzo-*p*-dioxin are strictly dependent on aryl hydrocarbon receptor activation in hemopoietic cells. *J. Immunol.* 160: 3844–3854.
45. Ishimaru, N., T. Yoneda, K. Saegusa, K. Yanagi, N. Haneji, K. Moriyama, I. Saito, and Y. Hayashi. 2000. Severe destructive autoimmune lesions with aging in murine Sjögren's syndrome through Fas-mediated apoptosis. *Am. J. Pathol.* 156: 1557–1564.
46. Kobayashi, M., N. Yasui, N. Ishimaru, R. Arakaki, and Y. Hayashi. 2004. Development of autoimmune arthritis with aging via bystander T cell activation in the mouse model of Sjögren's syndrome. *Arthritis Rheum.* 50: 3974–3984.
47. Kerkvliet, N. I., and J. A. Brauner. 1987. Mechanisms of 1,2,3,4,6,7,8-heptachlorodibenzo-*p*-dioxin (HpCDD)-induced humoral immune suppression: evidence of primary defect in T-cell regulation. *Toxicol. Appl. Pharmacol.* 87: 47–58.
48. Luster, M. I., D. R. Germolec, G. Clark, G. Wiegand, and G. J. Rosenthal. 1998. Selective effects of 2,3,7,8-tetrachlorodibenzo-*p*-dioxin and corticosteroid on in vitro lymphocyte maturation. *J. Immunol.* 140: 928–935.
49. Schmidt, J. V., G. H. Su, J. K. Reddy, M. C. Simon, and C. A. Bradfield. 1996. Characterization of a murine Ahr null allele: involvement of the Ah receptor in hepatic growth and development. *Proc. Natl. Acad. Sci. USA* 93: 6731–6736.
50. Gu, Y. Z., J. B. Hogenesch, and C. A. Bradfield. 2000. The PAS superfamily: sensors of environmental and developmental signals. *Annu. Rev. Pharmacol. Toxicol.* 40: 519–561.
51. Umannova, L., J. Zatloukalova, M. Machala, P. Kremar, Z. Majkova, B. Hennig, A. Kozubik, and J. Vondracek. 2007. Tumor necrosis factor-α modulates effects of aryl hydrocarbon receptor ligands on cell proliferation and expression of cytochrome P450 enzymes in rat liver "stem-like" cells. *Toxicol. Sci.* 99: 79–89.
52. Hoagland, M. S., E. Hoagland, and H. I. Swanson. 2005. The p53 inhibitor pifithrin-α is a potent agonist of aryl hydrocarbon receptor. *J. Pharmacol. Exp. Ther.* 314: 603–610.
53. Vogel, C. F., E. Sciullo, W. Li, P. Wong, G. Lazennec, and F. Matsumura. 2007. RelB, a new partner of aryl hydrocarbon receptor-mediated transcription. *Mol. Endocrinol.* 21: 2941–2955.
54. Vogel, C. F., E. Sciullo, and F. Matsumura. 2007. Involvement of RelB in aryl hydrocarbon receptor-mediated induction of chemokines. *Biochem. Biophys. Res. Commun.* 363: 722–726.
55. Gillard, G. O., and A. G. Farr. 2005. Contrasting models of promiscuous gene expression by thymic epithelium. *J. Exp. Med.* 202: 15–19.
56. Mandal, P. K. 2005. Dioxin: a review of its environmental effects and its aryl hydrocarbon receptor biology. *J. Comp. Physiol.* 175: 221–230.
57. Fan, F., B. Yan, G. Wood, M. Viluksela, and K. K. Rozman. 1997. Cytokines (IL-1β and TNFα) in relation to biochemical and immunological effects of 2,3,7,8-tetrachlorodibenzo-*p*-dioxin (TCDD) in rats. *Toxicology* 116: 9–16.
58. Vogel, C., S. Donat, O. Döhr, L. Kremer, C. Esser, M. Roller, and J. Abel. 1997. Effect of subchronic 2,3,7,8-tetrachlorodibenzo-*p*-dioxin exposure on immune system and target gene responses in mice: calculation of benchmark doses for CYP1A1 and CYP1A2 related enzyme activities. *Arch. Toxicol.* 71: 372–382.
59. Warren, T. K., K. A. Mitchell, and B. P. Lawrence. 2000. Exposure to 2,3,7,8-tetrachlorodibenzo-*p*-dioxin (TCDD) suppresses the humoral and cell-mediated immune responses to influenza A virus without affecting cytolytic activity in the lung. *Toxicol. Sci.* 56: 114–123.
60. Veldhoen, M., K. Hirota, A. M. Westendorf, J. Buer, L. Dumoutier, J. C. Renauld, and B. Stockinger. 2008. The aryl hydrocarbon receptor links TH17-cell-mediated autoimmunity to environmental toxins. *Nature* 453: 106–110.
61. Quintana, F. J., A. S. Basso, A. H. Iglesias, T. Korn, M. F. Farez, E. Bettelli, M. Caccamo, M. Oukka, and H. L. Weiner. 2008. Control of Treg and TH17 cell differentiation by the aryl hydrocarbon receptor. *Nature* 453: 65–72.

Structure-Activity–Dependent Regulation of Cell Communication by Perfluorinated Fatty Acids using *in Vivo* and *in Vitro* Model Systems

Brad L. Upham,[1] Joon-Suk Park,[1] Pavel Babica,[1] Iva Sovadinova,[1] Alisa M. Rummel,[1] James E. Trosko,[1] Akihiko Hirose,[2] Ryuichi Hasegawa,[2] Jun Kanno,[3] and Kimie Sai[3**]*

[1]Department of Pediatrics and Human Development, National Food Safety and Toxicology Center, Michigan State University, East Lansing, Michigan, USA; [2]Division of Risk Assessment, and [3]Division of Cellular and Molecular Toxicology, National Institute of Health Sciences, Tokyo, Japan

BACKGROUND: Perfluoroalkanoates, [e.g., perfluorooctanoate (PFOA)], are known peroxisome proliferators that induce hepatomegaly and hepatocarcinogenesis in rodents, and are classic nongenotoxic carcinogens that inhibit *in vitro* gap-junctional intercellular communication (GJIC). This inhibition of GJIC is known to be a function of perfluorinated carbon lengths ranging from 7 to 10.

OBJECTIVES: The aim of this study was to determine if the inhibition of GJIC by PFOA but not perfluoropentanoate (PFPeA) observed in F344 rat liver cells *in vitro* also occurs in F344 rats *in vivo* and to determine mechanisms of PFOA dysregulation of GJIC using *in vitro* assay systems.

METHODS: We used an incision load/dye transfer technique to assess GJIC in livers of rats exposed to PFOA and PFPeA. We used *in vitro* assays with inhibitors of cell signaling enzymes and antioxidants known to regulate GJIC to identify which enzymes regulated PFOA-induced inhibition of GJIC.

RESULTS: PFOA inhibited GJIC and induced hepatomegaly in rat livers, whereas PFPeA had no effect on either end point. Serum biochemistry of liver enzymes indicated no cytotoxic response to these compounds. *In vitro* analysis of mitogen-activated protein kinase (MAPK) indicated that PFOA, but not PFPeA, can activate the extracellular receptor kinase (ERK). Inhibition of GJIC, *in vitro*, by PFOA depended on the activation of both ERK and phosphatidylcholine-specific phospholipase C (PC-PLC) in the dysregulation of GJIC in an oxidative-dependent mechanism.

CONCLUSIONS: The *in vitro* analysis of GJIC, an epigenetic marker of tumor promoters, can also predict the *in vivo* activity of PFOA, which dysregulated GJIC via ERK and PC-PLC.

KEY WORDS: extracellular receptor kinase, gap-junctional intercellular communication, mitogen-activated protein kinase, perfluorooctanoate, perfluoropentanoate, phosphatidylcholine-specific-phospholipase C, tumor promotion. *Environ Health Perspect* 117:545–551 (2009). doi:10.1289/ehp.11728 available via *http://dx.doi.org/* [Online 23 October 2008]

Research on the environmental fate and toxicology of halogenated compounds has focused primarily on brominated and chlorinated organics, whereas fluorinated organics received less attention, partly because of the perception that these compounds, which are quite chemically inert, were also biologically inert (Key et al. 1997). However, perfluorinated fatty acids (PFFAs), such as perfluorooctanoate (PFOA) and perfluorooctane sulfonate (PFOS), are found in the environment and have been detected in the blood of animals throughout the world, including the seals of remote arctic regions, indicating widespread distribution (Kannan 2001; Tao 2006; Van de Vijver 2005). Significant levels of PFOA and PFOS have also been detected in the serum of humans, but there is evidence of a significant decline in body burdens of PFOS and PFOA over the last 5–10 years (Calafat et al. 2007). The values from the first National Health and Nutrition Examination Survey (NHANES) conducted from 1999 to 2000 reported geometric means of 30.4 μg PFOS/L and 5.4 μg PFOA/L, and the second NHANES conducted between 2003 and 2004 reported geometric means of 20.7 μg PFOS/L and 3.9 μg PFOA/L (Calafat et al. 2007). Contamination of the environment is not limited to PFOA and PFOS but also includes short-chain perfluorinated alkanoates, such as perfluorobutyrate, perfluoropentanoate (PFPeA), perfluorohexanoate, and perfluoroheptanoate (Skutlarek et al. 2006).

The acute toxicities of PFOA and PFOS in rodent systems are low (Hekster 2003; Kudo and Kawashima 2003). After the absorption of PFOA into the body, it is predominantly distributed in the liver and plasma and, to a lesser extent, the kidney and lungs (Kudo and Kawashima 2003). Thus, the chronic and short-term effects of PFOA in rats are found largely in the liver (Kennedy et al. 2004) and immune system (DeWitt et al. 2008). Peroxisome proliferation in rodent livers is one of the major responses to PFOA, along with subsequent interferences with normal metabolism of fatty acids and cholesterol, and the induction of hepatocellular hypertrophy (Kennedy et al. 2004). Peroxisome-proliferating chemicals are classic nongenotoxic tumor promoters in rodent liver tissue (Cattley et al. 1995), and like other peroxisome proliferators, PFOA has also been shown to strongly promote tumors in rodent livers (Abdellatif et al. 1991). However, peroxisome-proliferating compounds might not be strong tumor promoters in human livers because of species differences in the response to peroxisome proliferators *in vivo*, with rodents more responsive than primates (Klaunig et al. 2003).

Although the underlying mechanisms of tumor promotion might vary, such as the induction of peroxisome proliferation, tumorigenic cells have long been characterized as cells that lose their ability to regulate growth through contact inhibition (Borek and Sachs 1966) and lack the ability to terminally differentiate (Potter 1978), which implies a breakdown in one of the communicating mechanisms (Trosko and Upham 2005). Tumorigenic cells can be benign, leading to the compression of surrounding tissues, or have the potential to acquire genetic mutations that lead to a malignant state where the cancerous cells can invade surrounding tissues. Alteration of cell-to-cell communication via gap junctions has been implicated in the tumorigenic process and is supported by considerable evidence (Trosko and Ruch 2002).

Inhibition of gap-junctional intercellular communication (GJIC) appears to be a necessary, albeit insufficient, step of tumorigenesis and is therefore a common response of cells to tumor promoters, oncogenes, growth factors, and nongenotoxic carcinogens such as peroxisome proliferators (Trosko and Ruch 1998; Trosko and Upham 2005). Although GJIC is modulated by multiple signaling pathways, simple bioassays of intercellular communication can be used to assess dysregulation of gap junctions regardless of the upstream effectors.

Address correspondence to B.L. Upham, Michigan State University, 243 National Food Safety and Toxicology Center, East Lansing, MI 48824 USA. Telephone: (517) 884-2051. Fax: (517) 432-6340. E-mail: upham@msu.edu

*Current address: Division of Medical Safety Science, National Institute of Health Sciences, Tokyo, Japan.

**Current address: Division of Functional Biochemistry and Genomics, National Institute of Health Sciences, Tokyo, Japan.

This research was supported by National Institute of Environmental Health Sciences (NIEHS) grant R01 ES013268-01A2 to B.L.U. and by a Grant-in-Aid for Science Research from the Ministry of Education, Science, Sports, and Culture of Japan (11694334).

The contents of this article are solely the responsibility of the authors and do not necessarily represent the official views of the NIEHS.

The authors declare they have no competing financial interests.

Received 23 May 2008; accepted 23 October 2008.

Thus, GJIC is an excellent biomarker first to assess the potential tumorigenicity of chemicals and then to use as a cell signaling end point to determine the early molecular events induced by these chemicals.

Cell proliferative diseases, such as cancer, not only require the release of a quiescent cell from growth suppression via down-regulation of GJIC and/or changes in extracellular components (i.e., integrins), but also need to activate mitogenic signaling pathways. The mitogen-activated protein kinase (MAPK) pathways are the major intracellular signaling mechanisms by which a cell activates, via phosphorylation, transcription factors involved in mitogenesis (Denhardt 1996). The extracellular receptor kinase (ERK) pathway has been extensively characterized, is the most understood of the MAPK pathways (Denhardt 1996), and is a key pathway of carcinogenesis (Roberts and Der 2007).

In the present study, we extended our *in vitro* studies with F344 rat liver epithelial cells, which determined that PFOA, but not PFPeA, inhibited GJIC (Upham et al. 1998), to an *in vivo* study using F344 rats exposed to PFOA, PFPeA, or phenobarbital (PB), a known tumor promoter, to determine GJIC in liver tissue. We also continued our *in vitro* studies of PFOA versus PFPeA in determining differential effects of these compounds on MAPK, specifically ERK, and further determined that the mechanism of PFOA-induced inhibition of GJIC depends on redox activity, ERK, and phosphatidylcholine-specific phospholipase C (PC-PLC).

Materials and Methods

Chemicals. We purchased PFOA (purity > 90%) and PFPeA (purity = 97%), for the data presented in Figures 1–3 and 4A, from Fluka Chemie AG (Buchs, Switzerland), and because of unavailability from Fluka, we purchased PFOA for the data presented in Figures 4B, 5, and 6 from Aldrich Chemical Company Inc. (Milwaukee, WI, USA), with a purity of 96%. The purity values were obtained from the commercial sources. The ratios of linear versus branched isomers in our samples were undetermined. The stock solutions were prepared by dissolving the powder in the solvent: acetonitrile for the *in vitro* assays and dimethyl sulfoxide (DMSO) for the *in vivo* studies; we also used these solvents as the vehicle controls. We purchased Lucifer yellow (LY) from Molecular Probes (Eugene, OR, USA); sodium dodecyl sulfate, Tween 20, Tris, glycine, acrylamide, tetramethylethylenediamine (TEMED) and DC protein kit from Bio-Rad Laboratories (Hercules, CA, USA); DMSO, rhodamine-dextran (RhD; molecular weight, 10,000 Da), dithiothreitol (DTT), *N*-acetylcysteine (Nac), L-ascorbate-2-phosphate (Asc-2-P) sesquimagnesium salt hydrate, and PB from Sigma-Aldrich Chemical Company (St. Louis, MO, USA); D609 and U0126, from Tocris Bioscience (Ellisville, MO, USA); resveratrol from CTMedChem (Bronx, NY, USA); acetonitrile, from EM Science (Gibstown, NJ, USA); polyclonal antibodies directed to phospho-ERK, from New England Biolabs (Ipswich, MA, USA); and mouse polyclonal antibody directed to glyceraldehyde 3-phosphate dehydrogenase (GAPDH), from Chemicon (Temecula, CA, USA).

In vivo *study*. Animal treatment. The protocol for this study was approved by the Animal Care and Utilization Committee of the National Institutes of Health Sciences of Japan to assure that the rats were treated humanely and with regard for alleviation of suffering. Male Fischer-344 (F344) rats, 5 weeks old, were purchased from Charles River Japan (Kanagawa, Japan) and housed in plastic cages (five rats/cage). Male F-344 rats were chosen to match the *in vitro* studies that used liver epithelial cells isolated from male F-344 rats. The rats were kept under conditions of controlled temperature (23 ± 2°C), humidity (55 ± 5%), and lighting (12/12-hr dark/light cycle) and given CRF-12 basal diet (Oriental Yeast Co., Tokyo, Japan) and tap water *ad libitum*.

We used the rats in the experiments after 1 week of acclimation. Eighty rats were divided into four groups and twenty rats per group were treated with a single intraperitoneal (i.p.) administration of 100 mg/kg PFOA, 100 mg/kg PFPeA, 100 mg/kg PB, or only vehicle (DMSO). Four rats per group were killed under anesthesia at 1, 3, 6, 12, and 24 hr after administration. Another 16 rats were divided into four groups and four rats of each group were given powder diet containing PFOA, PFPeA, PB, or basal powder diet only (control), and then killed after 1 week. The diets were prepared by blending each chemical into the basal powder diet at final concentrations of 0.02% for PFOA and PFPeA and 0.05% for PB. We determined the weight of the rats at the beginning and end of the experiment, and the food consumption on days 3 and 7 of the experiment. Based on the average weight of the rats and the average food consumed per day, the estimated daily doses of chemical exposures for PFOA, PFPeA, and PB were 37.9, 32.3, and 93.3 mg/day/kg, respectively.

Diethyl ether was used to euthanize the rats. Before sacrifice, blood was collected from the orbital venous plexus under anesthesia with diethyl ether and prepared for measuring serum aspartate aminotransferase (sAST), serum alanine aminotransferase (sALT), and serum alkaline phosphatase (sALP). Determination of sAST, sALT, and sALP was carried out with a Hitachi automatic Analyzer 7150 (Hitachi, Ltd., Tokyo, Japan) using commercially available GOP, GPT and ALP diagnostic reagents (Wako Pure Chemical Industries, Ltd., Tokyo, Japan). After opening the abdominal cavity, we excised the liver and immediately used one part of the liver for the incision loading/dye transfer (IL/DT). Our preliminary study confirmed that the anesthetic and the vehicle, DMSO, under our experimental conditions did not affect *in vivo* GJIC.

Bioassay of GJIC (IL/DT). We assayed *ex vivo* GJIC in the liver by the IL/DT method described previously (Sai et al. 2000). A part of the left lobe of the liver was put on a plastic

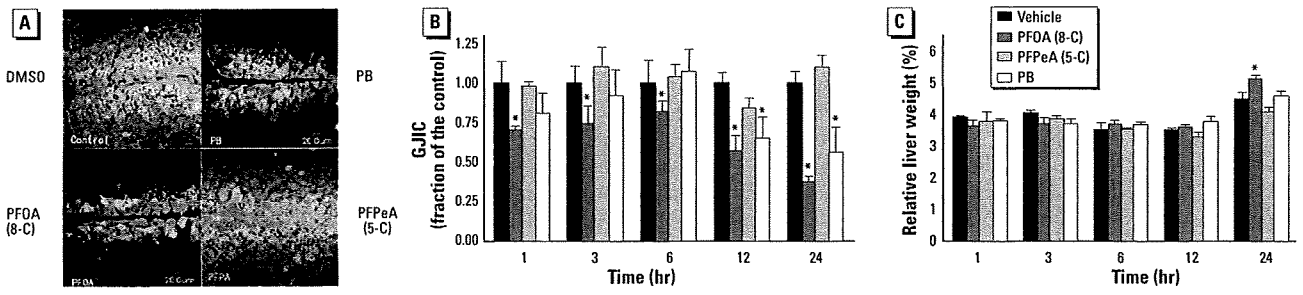

Figure 1. Analysis of *in vivo* effects of PFOA and PFPeA on GJIC in the liver tissue using IL/DT technique. Abbreviations: 5-C, five carbon; 8-C, eight carbon. (*A*) A fluorescent image of an IL/DT analysis of GJIC in the liver tissue of rats at 24 hr after a single i.p. administration of DMSO (vehicle), PB, PFOA, or PFPeA. Bar = 20 μm. (*B*) Mean + SD of the IL/DT data from rats treated with DMSO, PB, PFOA, or PFPeA for the acute exposure group. (*C*) Mean + SD relative liver weight from rats treated with DMSO, PB, PFOA, and PFPeA for the acute exposure group.
*$p < 0.05$ compared with vehicle, determined by one-way ANOVA for each time group followed by Dunnett's post hoc test.

plate covered with wet gauze. A mixture of fluorescent dyes containing 0.5 mg/mL LY and 0.5 mg/mL RhD in phosphate-buffered saline (PBS) was dropped on the tissue's surface. Three to four incisions were made on the surface of each specimen with a sharp blade. Excess amount of dye mixture was additionally put into the incisions and kept there for 3 min at room temperature. After incubation, the tissue was washed with PBS three times and fixed in 10% phosphate-buffered formalin overnight. Slices were washed with water and processed for embedding in paraffin. Five μm sections for GJIC analysis were prepared by cutting the paraffin block perpendicular to the incision line. Areas stained with LY alone or with RhD were detected by the emission of fluorescence using a confocal microscope (Fluoview, Olympus, Tokyo, Japan). We counted the number of cells stained with LY alone and normalized this number by dividing by the incision length. At least three incision sites per specimen were randomly chosen for the analysis, and the mean value was used as data from one animal. The values were expressed as a fraction of the control.

In vitro *study*. Cell culture. We obtained the WB-F344 rat liver epithelial cell line from J.W. Grisham and M.S. Tsao of the University of North Carolina at Chapel Hill, Chapel Hill, NC, USA (Tsao et al. 1984). Cells were cultured in D-medium (formula 78-5470EF, Gibco Laboratories, Grand Island, NY, USA), supplemented with 5% fetal bovine serum (Gibco Laboratories), and incubated at 37°C in a humidified atmosphere containing 5% CO_2 and 95% air. The cells were grown in 35-mm tissue culture plates (Corning Inc., Corning, NY, USA) and the culture medium was changed every other day. Bioassays were conducted with confluent cultures that were obtained after 2–3 days of growth.

These WB cells are diploid and nontumorigenic (Tsao et al. 1984) and have been extensively characterized for GJIC in the absence and presence of well-known tumor promoters, growth factors, tumor suppressor genes, and oncogenes (Trosko and Ruch 1998). Intrahepatic transplantation of WB cells, which are liver bipolar stem cells, into adult syngenic F344 rats results in the morphologic differentiation of these cells into hepatocytes and incorporation into hepatic plates (Coleman et al. 1993).

Bioassay of GJIC (scrape load/dye transfer). The scrape loading/dye transfer (SL/DT) technique was adapted after the method of Upham et al. (1998). The test chemicals were added directly to the cell culture medium from concentrated stock solutions. The migration of the dye through gap junctions was visualized with a Nikon Eclipse TE3000 phase contrast/fluorescent microscope and the images were digitally captured with Nikon EZ Cool Snap charge-coupled device camera (Nikon Inc., Nikon, Japan). GJIC was assessed by comparing the distance the dye traveled in the chemically treated cells with the distance the dye traveled in the vehicle controls, which was measured using the Gel-Expert imaging software (Nucleotech, San Mateo, CA, USA). We report GJIC as a fraction of the control. Based on previous results (Upham et al. 1996, 1998), 1-methylanthracene as well as PFOA were used as positive controls of inhibition of GJIC, whereas acetonitrile at vehicle concentrations was used as a negative control. The vehicles used for the *in vitro* assays, acetonitrile and PBS, had no effect on GJIC. We performed all experiments at least in triplicate and report the results as means ± SD at the 95% confidence interval.

Western blot analysis. Cells were grown in 35-mm-diameter Corning tissue culture plates to the same confluency as the SL/DT assay. The cells were depleted of serum 5 hr before addition of PFFAs to synchronize the cells into G_0 to minimize background ERK levels. This does not alter the effect on GJIC in the F344 WB cells, as previously determined (Rummel et al. 1999). The proteins were extracted with 20% sodium dodecyl sulfate (SDS) solution containing 1 mM phenylmethylsulfonyl fluoride, 100 μM Na_3VO_4, 100 nM aprotinin, 1.0 μM leupeptin, 1.0 μM antipain, and 5.0 mM NaF. The protein content was determined with the Bio-Rad DC assay kit. The proteins were separated on 12.5% SDS–polyacrylamide gel electrophoresis according to the method of Laemmli

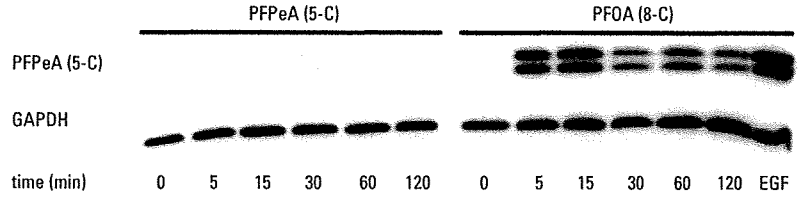

Figure 3. Activation of ERK-MAPK by PFOA, but not by PFPeA, in F344 WB rat liver epithelial cells determined by Western blots: Top panel probed with a phosphorylated ERK specific antibody and the bottom panel probed with a GAPDH specific antibody. The concentrations of PFPeA and PFOA were 100 μM. The concentration and time of incubation for epidermal growth factor (EGF) was 20.0 ng/mL and 15 min.

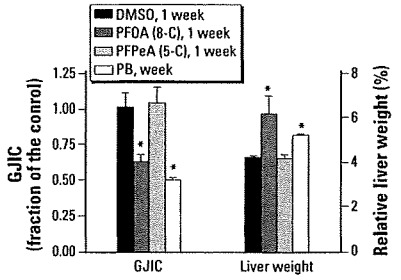

Figure 2. The long-term effects (1 week) of PB, PFOA, and PFPeA on GJIC and RLW (mean + SD). Abbreviations: 5-C, five carbon; 8-C, eight carbon. A one-way ANOVA was done for the GJIC data and a Kruskal-Wallis one-way ANOVA was done for the RLW data because these data failed the normality test.

*$p < 0.05$ compared with vehicle (DMSO); significant effects determined by ANOVA or Kruskal-Wallis ANOVA for each group was followed with a Dunnett's post hoc test at $p < 0.05$.

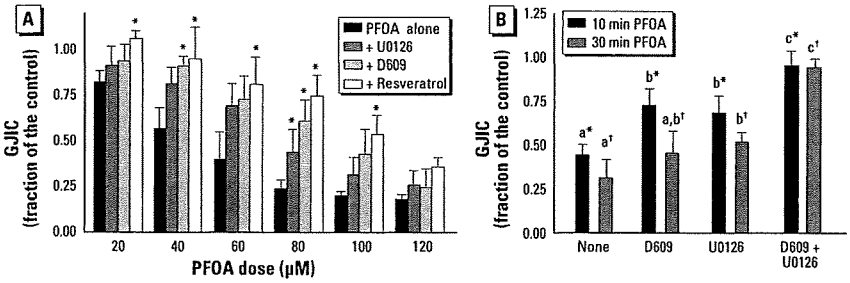

Figure 4. (*A*) Prevention of PFOA-induced inhibition of GJIC by inhibitors of MEK and PC-PLC and resveratrol at various doses of PFOA (mean + SD). The concentrations and times of preincubation of U0126, D609, and resveratrol were 20 μM/30 min, 50 μM/20 min, and 100 μM/15 min, respectively. A one-way ANOVA was done for each dose group. *Significant at $p < 0.05$ using the Dunnett's post hoc test that compared each inhibitor treatment with that of PFOA alone. (*B*) The interactive effect of MEK and PC-PLC inhibitors on reversing PFOA-induced inhibition of GJIC at 10 and 30 min (mean + SD). The concentrations and times of preincubation of U0126 and D609 were 20 μM/30 min and 50 μM/20 min, respectively. A one-way ANOVA indicated significance at $p < 0.05$ for each time group. The Tukey pairwise-comparison post hoc test was used to determine statistical differences, as indicated by different letters, between the inhibitor treatments for each time group. The lettered asterisks represent the 10-min group and lettered daggers represent the 30-min group.

(1970). Fifteen micrograms protein was loaded onto the gels and electrophoretically transferred from the gel to polyvinyl difluoride membranes (Millipore Corp., Bedford, MA, USA). Phosphorylated ERK 1 and ERK 2 were detected with a 1:2,000 dilution of anti-phospho-ERK polyclonal antibodies, and GAPDH was detected with a 1:10,000 dilution of anti-GAPDH polyclonal antibodies, that were incubated sequentially with the membranes, each for 2 hr. The protein–primary antibody complex was probed with a 1:1,000 dilution of horseradish peroxidase–conjugated anti-rabbit or anti-mouse antibodies (Amersham Life Science Products, Arlington Heights, IL, USA) for 1 hr. The ERK and GAPDH protein bands were detected using the Super Signal chemiluminescence detection kit (Pierce Corp., Arlington Heights, IL, USA), enhanced chemiluminescence (ECL) detection kit, and ECL Hyperfilm–MP (Amersham Life Science Products, Denver, CO, USA).

Statistics. For the *in vivo* studies, the value of each group was expressed as the mean ± SD of data derived from four rats. The *in vitro* assays were done in at least triplicate and expressed as a fraction of the control. The significance of differences in all results was evaluated with either a one-way analysis of variance (ANOVA) or, if the data set failed the normality test, a Kruskal-Wallis one-way ANOVA on ranked means. Normality assumption testing was done with the Kolmogorov-Smirnov test and equal variance assumption testing with the Levene median test. If ANOVA or Kruskal-Wallis ANOVA rejected the null hypothesis, then the results that were compared with a designated control used Dunnett's multiple-comparison post hoc tests or Tukey's post hoc test for pairwise multiple comparisons.

Results

In vivo *results.* The *in vivo* results of PFOA and PFPeA were compared with PB, a known liver tumor promoter. We used two different dosing schemes: an acute 24-hr exposure via i.p. administration and a longer-term (1 week) dietary exposure. An ANOVA indicated that PFOA, PFPeA, and PB had no statistically significant effect on body weights of the rats (data not shown). Liver injury was assessed using the biomarkers sALT, sAST, sALP, and the results for both dosing schemes are presented in Table 1. At day 7, there were no significant differences between the rats treated with PFOA, PFPeA, and PB for all three of the selected liver enzymes, indicating no long-term liver injury. After 1 day, we found a small, biologically insignificant, but statistically significant increase in sAST, with the data exhibiting high variability.

To assess the *in vivo* effects of these compounds on GJIC in the liver tissue, we used an IL/DT technique. Figure 1A shows the incorporation of the fluorescent dye into the liver cells and subsequent distribution of the fluorescent dye through the gap junctions of the tissue. RhD, which is a large-molecular-weight dye that does not traverse gap junctions, is color-coded red. LY, which does travel through gap junction channels, is color-coded from yellow for high intensity to green for lower intensity. We measured and averaged the distances traveled by the gap-junction–permeable dye and show them in Figure 1B (acute exposure) and Figure 2 (long-term exposure). PFOA and PB but not PFPeA inhibited *in vivo* GJIC in the liver tissues of rats treated either acutely or chronically. Significant inhibition of GJIC by PFOA was observed after 1 hr, and continued to inhibit GJIC until 24 hr in the acutely treated rats. Significant inhibition of GJIC did not begin until after 12 hr of treatment with PB in this group of rats.

In the acute dose regimen (Figure 1C), a significant increase in the relative weight of livers from rats treated with PFOA was observed at 24 hr. Similarly, rats chronically exposed to PFOA and PB for 1 week had significant increases in relative liver weight (RLW; Figure 2). The livers of animals treated either acutely or chronically with PFPeA did not significantly increase in relative weights compared with rats fed the vehicle (Figures 1C, 2).

In vitro *results.* Considering that the *in vitro* results of PFOA and PFPeA effects on gap junctions correlated with their effects on gap junctions *in vivo*, we did further *in vitro* analyses of PFOA to determine underlying mechanisms involved in the dysregulation of GJIC. PFOA, which inhibits GJIC, also activated ERK as determined by Western blot analysis of the phosphorylated, activated form of ERK (Figure 3). In contrast, the non-GJIC inhibitory PFPeA did not activate ERK (Figure 3). Activation of ERK was within 5 min in cells treated with PFOA, which correlates with the time of inhibition of GJIC, indicating a potential link. Preincubation of the cells with an MEK inhibitor, U0126, partially but significantly prevented the inhibition of GJIC by PFOA (Figure 4A). Preincubation of the cells with the PC-PLC inhibitor D609 also partially but significantly prevented the inhibition of GJIC by PFOA (Figure 4A). The significant contribution of PC-PLC and MEK in PFOA-induced inhibition of GJIC diminished after the maximum inhibitory dose of 80 μM to a nonsignificant involvement at the higher dose of 120 μM (Figure 4A), indicating further that mechanisms other than MEK and PC-PLC are also involved.

Gap junctions are known to be redox sensitive, so we conducted several experiments with various antioxidants. Resveratrol significantly reversed the inhibitory effect on GJIC and was possibly inhibiting both MEK and PC-PLC (Figure 4A). Additional experiments were performed to look at the combinatorial effect of pretreating cells with both D609 and U0126. The combination of both of these inhibitors of signal transduction enzymes resulted in the prevention of GJIC inhibition by PFOA, and the combinatorial effect was significantly greater than cells treated with either inhibitor alone as determined by a Tukey post hoc multiple-comparison test (Figure 4B). These results collectively indicate that PFOA-induced regulation of GJIC is a function of both of these signaling enzymes.

Further experiments were performed with DTT, Nac, and Asc-2-P (Figure 5). DTT

Table 1. The effect of PFOA, PFPeA, and PB on the levels of various biomarkers of liver injury in F344 rats.

Exposure, time, enzyme	Enzyme activity (mU/mL) DMSO (vehicle)	PFOA	PFPeA	PB
Acute (24 hr)				
sALT	51.5 ± 3.2	138.6 ± 126.4	56.3 ± 13.2	54.5 ± 4.1
sAST	98.8 ± 8.8	232 ± 169.8*	113.0 ± 17.6	100.6 ± 15.1
sALP	1672.8 ± 90.0	1521.8 ± 220.2	1495.0 ± 233.8	1561.0 ± 115.2
Longer-term (1 week)				
sALT	39.3 ± 2.0	41.2 ± 1.9	39.8 ± 3.0	39.7 ± 2.6
sAST	71.2 ± 10.0	70.4 ± 4.3	73.9 ± 10.7	76.1 ± 9.4
sALP	1488.8 ± 62.9	1394.5 ± 59.4	1449.5 ± 36.6	1349.3 ± 53.0

To determine significant effects, we performed a one-way ANOVA for sALP (1 day), sALP (1 week), and sALT (1 week) and a Kruskal-Wallis one-way ANOVA on ranks for sAST (1 day), sAST (1 week), and sALT (1 day). Any significant effects determined by ANOVA were followed by a Dunnett's post hoc test, with DMSO designated as the control.
*$p < 0.05$.

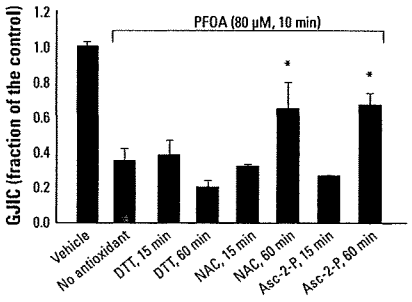

Figure 5. Prevention of PFOA-induced inhibition of GJIC by various antioxidants (mean + SD). The concentrations of PFOA, DTT, Nac, and Asc-2-P were 80 μM, 10 mM, 100 μM, and 100 μM, respectively.
*$p < 0.05$ by ANOVA and Dunnett's post hoc test comparing each antioxidant treatment with that of PFOA alone (no antioxidant).

and Nac in the absence of PFOA had no statistically (ANOVA) significant effect on GJIC at both 15 and 60 min (data not shown). Asc-2-P had a small, < 10% effect (ANOVA, Tukey) on GJIC in the absence of PFOA at 15 min but not 60 min (data not shown). Asc-2-P and Nac both prevented the inhibition of GJIC by PFOA within a 60-min preincubation time, but not DTT, implicating redox-sensitive proteins that probably do not involve thiol oxidations. Preincubation of Asc-2-P and Nac for 15 min did not reverse the effect of PFOA on GJIC. The oxidative nature of PFOA was not cytotoxic, as indicated after 2 days of growing cells after the log-phase of growth with 80 μM PFOA, resulting in no visual abnormalities in the morphology of the cells and complete restoration of GJIC after the cells were transferred to fresh medium for 5 hr containing no PFOA (Figure 6).

Discussion

Understanding the biological effects of the environmentally prevalent PFFAs on cell signaling pathways relevant to the epigenetic, nongenotoxic phase of cancer is important. In particular, GJIC offers a very central signaling system to assess risk (Trosko and Upham 2005). Although the transient closure of gap junction channels during proliferation is a normal response to mitogens, the chronic inhibition of GJIC by toxicants and toxins or by cytokines released during compensatory hyperplasia could lead to pathologic states (Trosko and Upham 2005; Upham and Trosko 2006). Thus, we conducted two dosing schemes, one a short term of 24 hr following an i.p. injection of PFOA, PFPeA, or PB, and another a longer-term study where the rats were dosed with these compounds through their daily feedings for 1 week. We previously demonstrated that inhibition of GJIC using *in vitro* model systems by perfluoroalkyl carboxylates and sulfonates depended on the chain length, where PFFAs with 7–10 carbons inhibited GJIC, and PFFAs with 2–6 carbons did not (Hu et al. 2002; Upham et al. 1998). To determine if chain length of PFFAs would exhibit similar effects on GJIC in a living organism, we treated F344 rats with PFOA, an eight-carbon PFFA, and PFPeA, a five-carbon PFFA, and determined GJIC in the liver tissue using an *ex vivo* IL/DT assay.

The liver is the primary target of PFOA (Kudo and Kawashima 2003), which is known to induce hepatocellular tumors in rodent model systems (Abdellatif et al. 1991; Kennedy et al. 2004). Similar to our *in vitro* results (Hu et al. 2002; Upham et al. 1998), PFOA decreased GJIC activity in the liver compared with the rats treated with the vehicle (control) for both the acute and long-term dosing schemes. In contrast, PFPeA-treated rats did not have altered GJIC in the livers compared with the control rats for both dosing schemes, which is also consistent with our *in vitro* observations. Another possible reason for the lack of an *in vivo* response by PFPeA could be a consequence of a greater elimination rate that is typical of PFFAs with shorter chain lengths (Chang et al. 2008; Ohmori et al. 2003). Although we did not measure the elimination rates of PFPeA in our experiments, the half-life of perfluorobutyrate is 9.2 hr (oral) and 6.4 hr (intravenous) in Sprague-Dawley rats (Chang et al. 2008). These half-lives are similar to that of PB in Sprague-Dawley rats, which is 8–9 hr. Considering that PB inhibited GJIC and induced hepatomegaly in the livers of the rats used in our experiments, and PFPeA did not inhibit GJIC using an *in vitro* assay system, we would expect that the noninhibitory effects of PFPeA on GJIC *in vivo* would not result from its increased rate of elimination. Further experiments are needed to confirm such a conclusion.

We previously published data that indicated the treatment of Sprague-Dawley rats with PFOS resulted in a decrease in GJIC activity in the liver tissue; thus, PFOA and PFOS have similar activities (Hu et al. 2002). The following are additional reports demonstrating that tumor promoters, known to inhibit GJIC *in vitro*, also inhibited GJIC *in vivo*: pentachlorophenol (Sai et al. 2000), 2-acetylaminofluorene (Krutovskikh et al. 1991), PB (Kolaja et al. 2000; Krutovskikh 1995), polychlorinated biphenyls (Kolaja et al. 2000; Krutovskikh 1995), pregnenolone-16α-carbonitrile (Kolaja et al. 2000), cadmium (Jeong et al. 2000), clofibrate, and DDT (Krutovskikh 1995). Another interesting report on the *in vivo* effects of chemicals on GJIC is the treatment of rats with the antioxidants lycopene and alpha and beta carotene. High doses of these antioxidants resulted in a decrease in GJIC activity, whereas rats exposed to low doses exhibited an increase in GJIC (Krutovskikh et al. 1997). Although *in vivo* assessment of intercellular communication has been limited in both the number of studies and choice of organ, namely, the liver, these results, including those presented in this report, nevertheless suggest that the *in vitro* rat liver epithelial cell assay system is a good predictor of the *in vivo* effects of chemicals on gap junctions in the liver tissues of rodents.

PFOA and PB induced hepatomegaly, whereas PFPeA had no effect. These results are similar to those previously published indicating that PFOA, but not perfluorobutyrate, affected RLWs in F344 rats (Takagi et al. 1991). Although not causally linked, hepatomegaly has been correlated with the promotion of liver tumors by many peroxisome proliferator-activated receptor α agonists, including PFOA (Takagi et al. 1992). The null effect of PFPeA on GJIC and hepatomegaly suggest that PFPeA would not be a tumor promoter; however, two-stage (initiation and promotion) carcinogenesis studies would be needed to confirm this conclusion. Tissue necrosis is known to induce compensatory hyperplasia that leads to increased liver weights, but this is unlikely the cause of hepatomegaly in the PFOA- and PB-treated rats, considering that no visual damage of the liver was seen in the histologic sections (data not shown) and there was no increase in serum enzymes.

Tissue homeostasis in multicellular organisms depends on functional GJIC, and the disruption of intercellular communication has been linked to many diseases (Trosko and Upham 2005). PFOA clearly interrupted GJIC in the liver tissues of rats, but further experiments would need to be done in other species. PFOS also inhibited GJIC in rat liver tissue as well as *in vitro* systems that included dolphin kidney cells (Hu et al. 2002). Thus, the potential for cross-species effects of PFOA on GJIC implicates a health risk to multicellular organisms. Future experiments, particularly with human cell lines, will aid in determining differences in the sensitivity of various organisms to the effects of PFOS and PFOA on GJIC and allow for more accurate assessment of risks these compounds pose to humans and wildlife.

Considering that *in vitro* analyses of PFFA, using rat liver epithelial cells, accurately predicted the *in vivo* effects on GJIC for various PFFAs, we did further *in vitro* analyses of PFPeA- and PFOA-treated rat liver epithelial cells to determine potential signaling mechanisms involved in PFOA-induced regulation of GJIC. Connexin 43 (Cx43) is a

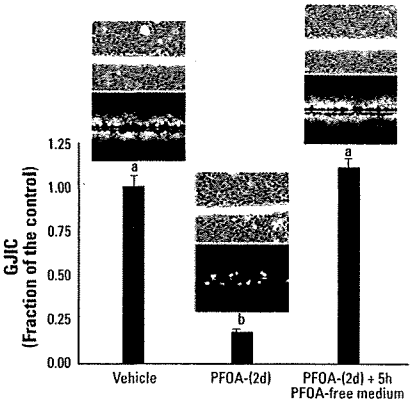

Figure 6. The effects of an extended incubation of cells with PFOA (80 μM, 2 days) and transfer of cells to PFOA-free medium (5 hr) on cell morphology and GJIC (mean + SD). Each phase-contrast and fluorescent photomicrograph represents one of the three replicates of each treatment group (magnification, 200×). Different letters indicate significance at $p < 0.05$ using ANOVA and Tukey post hoc test with a pairwise comparison.